ANKARA YILDIRIM BEYAZIT UNIVERSITY

GRADUATE SCHOOL OF NATURAL AND APPLIED SCIENCES



LOW-COST PERIMETER INTRUSION RADAR DEVELOPMENT

M.Sc. Thesis by

Ahmet İNANÇ

Department of Electrical and Electronics Engineering

September, 2020

ANKARA

LOW-COST PERIMETER INTRUSION RADAR DEVELOPMENT

A Thesis Submitted to

The Graduate School of Natural and Applied Sciences of

Ankara Yıldırım Beyazıt University

In Partial Fulfillment of the Requirements for the Degree of Master of Science in Electrical and Electronics Engineering, Department of Electrical and Electronics Engineering

by

Ahmet İNANÇ

September, 2020

ANKARA

M.Sc. THESIS EXAMINATION RESULT FORM

We have read the thesis entitled **"LOW-COST PERIMETER INTRUSION RADAR DEVELOPMENT"** completed by **AHMET İNANÇ** under the supervision of **PROF. DR. ASAF BEHZAT ŞAHİN** and we certify that in our opinion it is fully adequate, in scope and in quality, as a thesis for the degree of Master of Science.

Prof. Dr. Asaf Behzat ŞAHİN

Supervisor

Prof. Dr. Hakan ALTAN

Jury Member

Doç. Dr.Enver ÇAVUŞ

Jury Member

Prof. Dr. Ergün ERASLAN

Director

Graduate School of Natural and Applied Sciences

I hereby declare that, in this thesis which has been prepared in accordance with the Thesis Writing Manual of Graduate School of Natural and Applied Sciences,

- All data, information and documents are obtained in the framework of academic and ethical rules,
- All information, documents and assessments are presented in accordance with scientific ethics and morals,
- All the materials that have been utilized are fully cited and referenced,
- No change has been made on the utilized materials,
- All the works presented are original,

and in any contrary case of above statements, I accept to renounce all my legal rights.

Date: **Signature:……..**

Name & Surname: Ahmet İNANÇ

ACKNOWLEDGMENTS

Firstly, I would like to express my sincere gratitude to my supervisor, Prof. Dr. Asaf Behzat ŞAHİN, for his tremendous support and motivation during my study. His immense knowledge and precious recommendations constituted the milestones of this study. His guidance assisted me all the time in my research and while writing this thesis.

I would express my deep appreciation to my parents, sisters, and brothers who always supported and encouraged me throughout my life.

I would like to thank my dear wife for all her sacrifice and understanding. I cannot imagine how I would be successful without her support.

Lastly, this thesis is dedicated to my little coming soon.

2020, 08 September Ahmet İNANÇ

LOW-COST PERIMETER INTRUSION RADAR DEVELOPMENT

ABSTRACT

In this thesis, a very low-cost perimeter intrusion radar system is developed by using X-Band Microwave Motion Sensor Module called HB-100. When the 5-Volt input supply voltage of the sensor was modulated with a triangular wave, a 3 MHz difference in output frequency between 10525 - 10528 MHz was detected, which means that the sensor can be used as an FMCW radar and the distance information of the stationary target can be obtained. In Perimeter Intrusion Detection Systems (PIDS), it is essential to know not only the intrusion in the protected area but also the distance of the intruders. Civil application radars, which can detect people from distances of more than 1 kilometer, can be purchased with a very high budget. However, using the sensor's internal receiver and the designed external lens, one kilometer away target can be detected at a much cheaper cost. The development of low-cost radar is a very innovative issue due to the lack of civilian PIDS that can detect people beyond kilometers. Also, by operating a Doppler radar sensor, which can be obtained for less than 5 USD as an FMCW radar, it will be possible to detect people from long distances and save a hundred or even thousand times of budget. The target detection range is an essential concept in PIDS. Lens specifications designed to increase target detection range are given. Theoretical calculations of the maximum range for the sensor's internal receiver and external lens have been made. It has been calculated that the maximum range is increased approximately ten times with the externally designed lens. Besides, according to the specified characteristics of the sensor, calculated and simulated Intermediate Frequency (IF) - range relationship is presented. The calculated and simulated values were confirmed by laboratory measurements, and results graphics are presented.

Keywords-Perimeter Intrusion Radar; FMCW Radar; HB-100 Motion Sensor; Low-Cost Radar Sensor

DÜŞÜK BÜTÇELİ ÇEVRE SALDIRI TESPİT RADARI GELİŞTİRİLMESİ

ÖZ

Bu tezde, HB-100 adı verilen X-Band Mikrodalga Hareket Sensörü Modülü kullanılarak çok düşük maliyetli bir çevre saldırı tespit radar sistemi geliştirilmiştir. Sensörün 5 Volt giriş besleme gerilimi bir üçgen dalga ile modüle edildiğinde, 10525 - 10528 MHz arasındaki çıkış frekansında 3 MHz'lik bir fark tespit edildi, bu da sensörün FMCW radarı ve mesafe bilgisi olarak kullanılabileceği ve sabit hedefin mesafe bilgisinin elde edilebileceği anlamına gelir. Çevre Saldırı Tespit Sistemlerinde (ÇSTS), yalnızca korunan alandaki izinsiz girişleri değil, aynı zamanda izinsiz girenlerin mesafesini de bilmek önemlidir. 1 kilometreden fazla mesafeden insanları tespit edebilen sivil uygulama radarları çok yüksek bir bütçe ile satın alınabilir. Bununla birlikte, sensörün dahili alıcısı ve tasarlanan harici lens kullanılarak, bir kilometre uzaktaki hedef çok daha ucuz bir maliyetle tespit edilebilir. Düşük maliyetli radarın geliştirilmesi, kilometre ötesi insanları tespit edebilen sivil ÇSTS eksikliği nedeniyle çok yenilikçi bir konudur. Ayrıca, 5 USD'nin altında bir fiyata elde edilebilen bir Doppler radar sensörünün bir FMCW radar olarak çalıştırılmasıyla, insanları uzun mesafelerden tespit etmek ve bütçeden yüz hatta bin kat tasarruf etmek mümkün olacaktır. Hedef tespit menzili, ÇSTS' de önemli bir kavramdır. Hedef tespit menzilini artırmak için tasarlanmış lens özellikleri verilmiştir. Sensörün dahili alıcısı ve harici lensi için maksimum menzilin teorik hesaplamaları yapılmıştır. Harici olarak tasarlanan lens ile maksimum menzilin yaklaşık on kat arttığı hesaplanmıştır. Ayrıca sensörün belirlenen özelliklerine göre hesaplanan ve simüle edilen Ara Frekans (IF) - menzil ilişkisi sunulmuştur. Hesaplanan ve simüle edilen değerler, laboratuvar ölçümleri ile doğrulanmış ve sonuç grafikleri sunulmuştur.

Anahtar Kelimeler: Çevre Saldırı Tespit Radar; FMCW Radar; HB-100 Sensör; Düşük Bütçeli Radar Sensör

CONTENTS

M.Sc. THESIS EXAMINATION RESULT FORM ii
ETHICAL DECLARATION iii
ACKNOWLEDGMENTS iv
ABSTRACT v
ÖZ vi
NOMENCLATURE ix
LIST OF TABLES xii
LIST OF FIGURES xiii
CHAPTER 1 - INTRODUCTION 1
1.1 General Overview 1
1.2 The Aim of Study and Motivation 2
1.3 Organization of Thesis 3
1.4 Literature Review 4
CHAPTER 2 - BACKGROUND 5
2.1 Radar Systems 5
2.2 Theory of CW Radar 10
2.2.1 Doppler Radar and Velocity Calculation 11
2.3 Fundamentals of FMCW Radar 13
CHAPTER 3 - EXPERIMENTAL SETUP 21
3.1 HB-100 Sensor 21
3.1.1 General Description 21
3.1.2 Antenna Specifications 23
3.1.3 Use of HB100 Sensor as FMCW radar 26
3.2 Lens Design 27
3.2.1 Lens Specification 28
3.2.2 Conservation of étendue 31
3.3 Explanation of the General System 34
CHAPTER 4 - THEORETICAL CALCULATIONS 35
4.1 System Parameters for Maximum Detection Range Calculations 35
4.1.1 HB100 Sensor Specification 35
4.1.2 Antenna Parameters 36
4.2 FMCW Radar Maximum Detection Range Calculations 37

4.2.1 Calculation of Max. Det. Range without Using an External Lens 38
4.2.1.1 Beamwidth Calculation without Using External Lens 40
4.2.2 Calculation of Maximum Detection Range Using 20 cm Lens 41
4.2.2.1 Beamwidth Calculation Using 20 cm Lens 42
4.2.3 Calculation of Maximum Detection Range Using 40 cm Lens 42
4.2.3.1 Beamwidth Calculation Using 40 cm Lens 43
4.2.4 Calculation of Range Accuracy 44
CHAPTER 5 - MEASUREMENT AND RESULTS 45
CHAPTER 6 - DISCUSSION AND CONCLUSION 54
REFERENCES 55
APPENDICES 59
Appendix A – IEEE Standard Letter Designations for Radar Bands 59
Appendix B – MATLAB Code for IF-Range Simulation 60
Appendix C – MATLAB Code for Expected - Simulated Max. IF Frequency . 61
Appendix D – MATLAB Code for Laboratory Measurements at 12 meters 63
CURRICULUM VITAE 65

NOMENCLATURE

Roman Letter Symbols

R	Range, m
c	Speed of light, m/s
f_b	Beat frequency, Hz
f_c	Center frequency of transmitted signal, Hz
f_d	Doppler frequency, Hz
f_{Tx}	Transmit frequency, Hz
f_{Rx}	Receiver frequency, Hz
T_m	Triangular signal period, s
V_r	Relative speed of the target, m/s
P_T	Power of transmitter, W
P_R	Received Power, W
σ	Radar Cross Section, m^2
S_s	Scattered power density
S_i	Incident power density
P_N	Noise Power, W
k_b	Boltzmann's constant (1.38x10-23 Ws/K),
T_s	System noise temperature
β	Bandwidth, Hz
λ	Wavelengths
N_w	Number of wavelengths
A_{exc}	Total angle of excursion
ω	Angular frequency
ϕ	Phase angle

f_d	Doppler frequency
V_r	Relative velocity
f_c	Chirp start frequency
T_c	Chirp duration
S	Slope
P_t	Transmitted Power,
G_t	Transmit Antenna Gain,
G_r	Receive Antenna Gain,
λ	Wavelength of Radar Signal,
k	Boltzmann's Constant (1.38×10^{-23} J/K),
T	Absolute Temperature of The Receiver Input (290 °K),
F	Noise Factor
θ_h	Horizontal Beamwidth
θ_v	Vertical Beamwidth
D_{b1}	Diameter of The Internal Antenna
D_{b2}	Diameter of The Designed Lens
Bw_{a1}	Beamwidth of The Internal Antenna
Bw_{a2}	Beamwidth of The System with The Lens
d_{ap}	Minimum Aperture Width
S_r	Range Resolution

Greek Letter Symbols

τ	Propagation Delay
β	Bandwidth, Hz
ϵ	Etendue

Subscripts

max	Maximum
min	Minimum

Acronyms

PIDS	Perimeter Intrusion Detection Systems
EO	Electro - Optical
FMCW	Frequency Modulated Continuous Wave
RF	Radio - Frequency
CW	Continuous-Wave
RCS	Radar Cross Section
SNR	Signal to Noise Ratio
IF	Intermediate Frequency
ADC	Analog to Digital Converters
DRO	Dielectric Resonator Oscillator
ITU	International Telecommunication Union
LPF	Low - Pass Filter
EIRP	Equivalent Isotropic Radiated Power
HDPE	High-Density Polyethylene

LIST OF TABLES

Table 2.1 RCS for Typical Targets at X-band 8
Table 3.1 HB-100 Sensor Specification 23
Table 3.2 Sensor parameters to be used in FMCW radar calculations 27
Table 4.1 HB100 Sensor Parameters 36
Table 4.2 Antenna Gain Calculation 36
Table 4.3 System Parameters 38
Table 4.4 Maximum Range and Beamwidth Values 44
Table 5.1 Expected and Simulated Maximum IF values 45

LIST OF FIGURES

Figure 1.1 Calculated Atmospheric Attenuation in the IR band 2

Figure 2.1 Radar Operating Principle 5

Figure 2.2 RCS Illustration 6

Figure 2.3 Classification of Radar System by Waveform 9

Figure 2.4 Structure of CW Radar Systems 10

Figure 2.5 Doppler Effect 11

Figure 2.6 Radial Velocity of Moving Target 13

Figure 2.7 Block Diagram of FMCW Radar 14

Figure 2.8 (a) A Sinusoidal Chirp Signal **(b)** Frequency vs Time Representation of Chirp Signal 15

Figure 2.9 Working Principle of Mixer 16

Figure 2.10 Transmitted and Received Signals and Corresponding IF Signal When A Single Object is in front of The Antenna 17

Figure 2.11 (Top) Instantaneous frequency of transmitted and received waves in case of a single stationary object. (Bottom) Resulting beat frequency. 18

Figure 2.12 Transmitted, two received signals (modulation frequency) and two beat frequencies according to the received signals. 20

Figure 3.1 HB-100 Doppler Sensor Module 21

Figure 3.2 HB-100 Doppler Radar Block Diagram 22

Figure 3.3 Internal Structure of the HB100 Sensor 22

Figure 3.4 Antenna Beam Pattern of HB-100 Sensor 24

Figure 3.5 HB-100 sensor test 25

Figure 3.6 HB-100 sensor measured EIRP Pattern 26

Figure 3.7 Designed Lens for Antennas 28

Figure 3.8 Beam Spot Diagram 29

Figure 3.9 Beam Lens Radiation Pattern 30

Figure 3.10 Visualization of etendue 32

Figure 3.11 Simplified Visualization of 3D etendue..... 33

Figure 3.12 Test Setup..... 34

Figure 4.1(a) Beamwidth for 122 m **(b)** Beamwidth for 32,5 m..... 41

Figure 4.2 (a) Beamwidth for 1440 m **(b)** Beamwidth for 650 m..... 42

Figure 4.3 (a) Beamwidth for 4870 m **(b)** Beamwidth for1296 m..... 43

Figure 5.1 Expected and Simulated Maximum IF values 46

Figure 5.2 Receiver IF Response (dBm) – Frequency Graph @ 1 meter 47

Figure 5.3 Receiver IF Response (dBm) – Frequency Graph @ 2 meters……47

Figure 5.4 Receiver IF Response (dBm) – Frequency Graph @ 5 meters..... 48

Figure 5.5 Receiver IF Response (dBm) – Frequency Graph @ 10 meters……..48

Figure 5.6 Receiver IF Response (dBm) – Frequency Graph @ 20 meters..... 49

Figure 5.7 Receiver IF Response (dBm) – Frequency Graph @ 50 meters..... 49

Figure 5.8 Receiver IF Response (dBm) – Frequency Graph @ 100 meters..... 50

Figure 5.9 Receiver IF Response (dBm) – Frequency Graph @ 200 meters..... 50

Figure 5.10 Receiver IF Response (dBm) – Frequency Graph @ 500 meters..... 51

Figure 5.11 Receiver IF Response (dBm) – Frequency Graph @ 1000 meters……51

Figure 5.12 Calculated and Simulated Maximum IF Frequency Results..... 52

Figure 5.13 Laboratory measurements at 12 meters 53

Figure 5.14 Response Difference 1st and 2nd Harmonic..... 53

CHAPTER 1

INTRODUCTION

1.1 General Overview

Perimeter Intrusion Detection Systems (PIDS) are a crucial part of most physical security systems. The protection of critical infrastructure is a growing concern within the high-security sensitive areas. Recently, PIDS have been widely used for critical infrastructure protection such as border security, government building security, airport security, railway and oil pipeline security, wide-area surveillance, etc. Radar, Electro-Optical (EO), acoustic, etc. sensors can be used for PIDS according to the requirement. Radars are generally used for these systems, and they are indispensable in integrated systems. In PIDS systems, it is essential to know not only the intrusion in the protected area but also the distance of the intruders. In most civilian applications, the target's distance from the radar is ignored due to the budget. FMCW (Frequency Modulated Continuous Wave) radars must be used to determine the distance to the target. The cost of these radars, which are more complex than other simple sensors, is higher than other simple radars such as Doppler radar. At this point, obtaining FMCW radar with low cost draws attention as an innovative and useful issue. Besides, there is no low-budget radar developed for civil applications that can detect people from long distances beyond kilometers and provide distance information of the detected person. The use of existing military radars in civilian applications is not cost-effective, and military systems are challenging to obtain.

The main reason why radars are preferred more than other sensors in PIDS is that they are not affected by weather conditions and climatic conditions. In addition, due to the low atmospheric attenuations of radars, target detection distances are higher than cameras and other systems. In figure 1.1 below, atmospheric losses in different weather conditions such as rain, fog, and ambient conditions are shown. Since the radar sensor used in this thesis operates in X-band, attention should be paid to the 10 GHz part in the graph. When the relevant section is examined, it is seen that atmospheric attenuations at 10 GHz are relatively low compared to other frequency values.

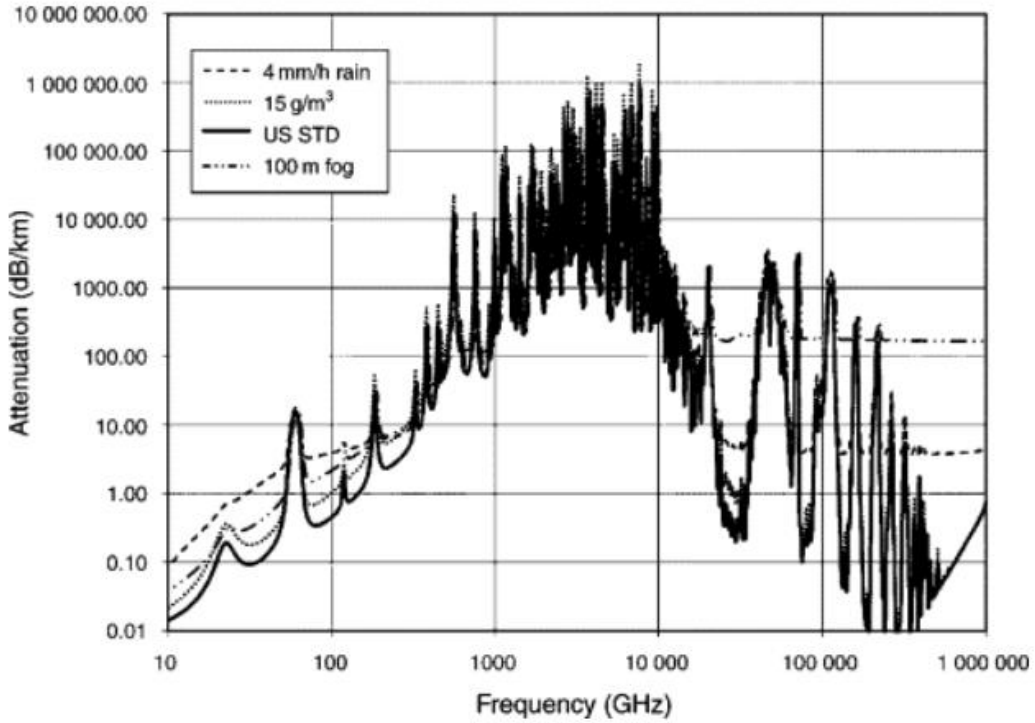


Figure 1.1 Calculated Atmospheric Attenuation in the IR band [1]

1.2 The Aim of Study and Motivation

In this thesis, it is aimed to develop a low-cost Perimeter Intrusion Radar (PIR) by using X-Band Microwave Motion Sensor Module called HB-100. However, the distance information of the detected target cannot be obtained with this low budget doppler motion radar sensor. Therefore, our primary motivation in the thesis is to use the HB100 Doppler radar sensor as a Frequency Modulated Continuous Wave (FMCW) Radar. Thus, it is aimed to show that the distance information of the target can be obtained.

Besides, the point to be emphasized is that civil application radars, which can detect people from distances of more than 1 kilometer, can be purchased with a very high budget. However, using the sensor's internal receiver and the designed external lens, one kilometer away target can be detected at a much cheaper cost.

The development of low-budget radar is a very innovative issue due to the lack of civilian PIR systems that can detect people beyond kilometers, and the existing military systems cannot be provided due to a very high budget. Also, by operating a Doppler radar sensor, which can be obtained for less than 5 USD as an FMCW radar, it will be possible to detect people from long distances and save a hundred or even thousand times of budget.

1.3 Organization of Thesis

This thesis consists of six chapters, as follows:

Chapter 1 includes general overview sections where general PIR systems are introduced; after that, the aim of the thesis and organization of the dissertation are explained. Lastly, the literature review is presented.

In Chapter 2, the basic radar theory is introduced. The doppler radar and FMCW radar theory are explained in detail. Other theoretical issues related to radar systems that constitute the basis of the thesis and are useful to know are presented.

In Chapter 3, the experimental setup, including the X-Band Microwave Motion Sensor Module, called HB100, and the designed external lens is introduced. The sensor's internal antenna parameters and designed external lens parameters have been explained. Calculation of antenna gain according to antenna azimuth and elevation beamwidth is explained. Besides, the conservation etendue principle, which increases the antenna gain by decreasing the antenna beamwidth, was described.

In Chapter 4, Theoretical calculations were made for the maximum detection range. Antenna gains were calculated according to whether an external lens is used or not in the system. Maximum Range and beamwidth values were calculated for all situations according to the determined antenna gains.

In Chapter 5, measurements and results are presented. In this context, the relationship between IF and range was calculated and simulated. The frequency of IF was calculated and simulated for 1,2,5,10,20,50,100,200,500 and 1000 meters, respectively. Expected and Simulated Maximum IF values were obtained as a result of the Matlab simulation. And also, The data obtained in the test setup in the laboratory were processed, and it was shown that the theoretical calculations were consistent in practice.

In Chapter 6, the conclusion and future works are described. It is explained that the theoretical calculations, simulations, and laboratory tests made with the designed system parameters are consistent. In addition, improvements to be made in order to use the system in real applications are explained in the future works section.

1.4 Literature Review

The history of perimeter protection is based on building fences. That primary concept evolved into perceiving activity along the fences using a variety of sensors [2,3]. Nowadays, it is not enough to build a fence, but it is also necessary to provide fence security with various precautions. A wide variety of sensors are available to mount on a fence, as well as many different types of Infrared, radar, Electro-Optical (EO), acoustic sensors, etc. Among them, radars are more preferred because they are not affected by weather and light conditions [4]. In addition to single-sensor systems, there are also integrated perimeter security systems using both camera and radar technologies with sensor fusion techniques [4,13]. In those systems, in order to decrease false alarm rate, target tracking and object recognition algorithms have been studied, and radar - EO sensor fusion techniques are applied [5,7]. Although optical equipment is efficient, changes in lighting and weather conditions reduce the system performance. For these reasons, radar systems are more widely used for perimeter intrusion detection systems [6]. In addition to detecting targets with radar, distance information of the target is also important. Hence, Frequency Modulated Continuous Wave (FMCW) Radar is used for distance information of the target. [9,13,15,16]

In this study, a very low-cost perimeter intrusion radar system is developed by using X-Band Microwave Motion Sensor Module called HB-100. Although this sensor is a Doppler radar module, we used this sensor as the FMCW Radar, which provides distance information of the target. Civil application radars, which can detect people from distances of more than 1 kilometer, can be purchased with a very high budget. However, using the sensor's internal receiver and the designed external lens, one kilometer away target can be detected at a much cheaper cost.

CHAPTER 2

BACKGROUND

2.1 Radar Systems

Although the scope of the thesis is related to the FMCW radar, the basic radar concept must be understood to evaluate the performance of the developed radar. As shown in Figure 1, the Radio-Frequency (RF) signal is transmitted to the object, and scattered power from the object called an echo signal, is received with radar. The radar system uses this echo signal to specify the velocity, direction, and distance of the reflecting target.

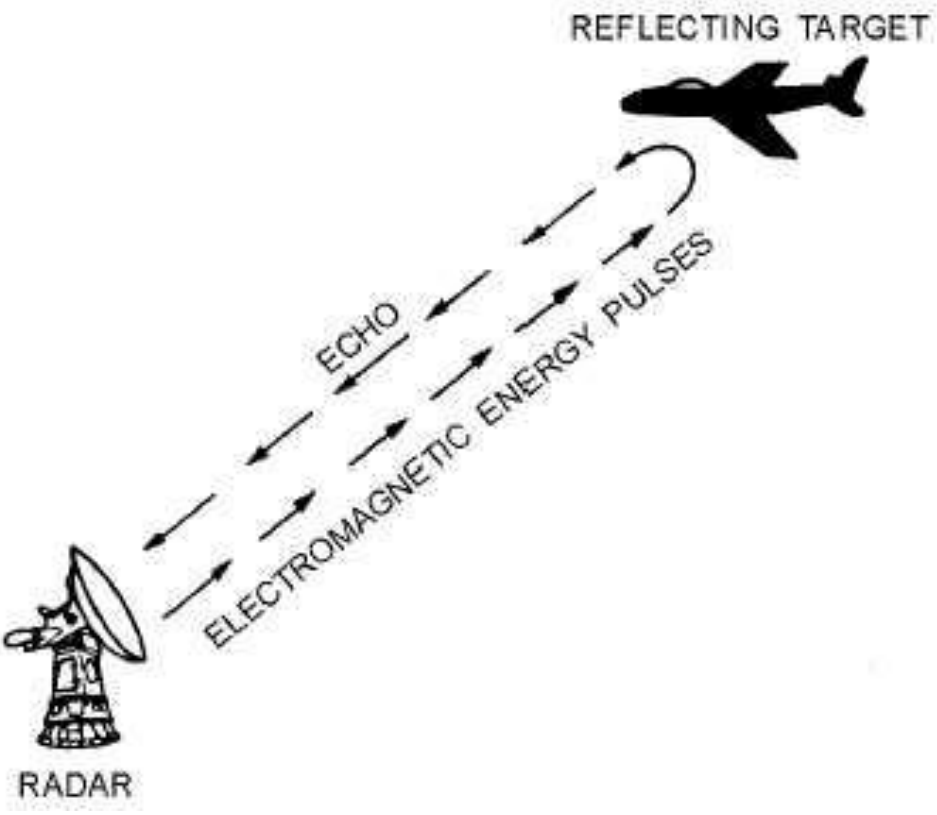


Figure 2.1 Radar Operating Principle

According to the number of antennas, radars are separated into two as monostatic and bistatic. Although the number of antennas used is different, the general radar equations are almost the same for both types. If the radar system has two antennas, that is, bistatic radar, the antenna gain is expressed in G_T and G_R Where G_T and G_R are the gain of the transmitter and receiver antennas. Since monostatic radar systems have a single antenna, the transmitter and receiver

antennas are only expressed in G. In general radar equation, the power density (watts per unit area) at a distance R can be calculated with equation 2.1.

$$P_d(R) = \frac{P_T G}{4\pi R^2} \tag{2.1}$$

where P_T is the power of the radar transmitter, G is antenna gain. The received power (P_R), which is dependent on the power density at the receiving site and the effective antenna aperture at the receiver, can be calculated as given in equation 2.2.

$$P_R = \frac{P_T G^2 \lambda^2}{(4\pi)^3 R^4} \sigma \tag{2.2}$$

where σ is Radar Cross-Section, which is an expression of how perceptible an object is by radar, and it is expressed in square meters. In this dissertation, since PID radar development is intended, it is crucial to determine the RCS values of possible targets. RCS is calculated as given in equation 2.3.

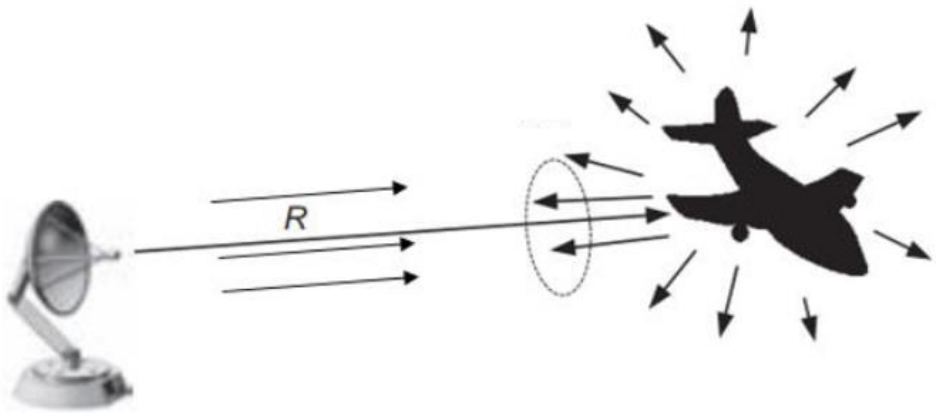


Figure 2.2 RCS Illustration

$$\sigma = \lim_{R\to\infty} 4\pi R^2 \frac{S_s}{S_i} \tag{2.3}$$

where Ss is scattered power density, and Si is incident power density. In the radar equation, system losses should be taken into account in order to calculate the maximum range. Hence, Signal to Noise Ratio (SNR) can be calculated as given in equation 2.4.

$$SNR = \frac{P_R}{P_N} \tag{2.4}$$

where P_N denotes the noise power, and it is expressed by the thermal noise, which is presented in equation 2.5.

$$P_N = k_b T_s \beta \tag{2.5}$$

In the equation given above, k_b is Boltzmann's constant ($1.38\text{x}10^{-23}$ Ws/K), T_s is the system noise temperature and β is the instantaneous receiver bandwidth in Hz. If the P_N value is substituted on equation 4, (SNR) can be calculated as given in equation 2.6.

$$SNR = \frac{\sigma P_T G^2 \lambda^2}{(4\pi)^3 R^4 k_b T_s \beta} \tag{2.6}$$

From the equation above, the range formula in equation 2.7 is obtained.

$$R = \sqrt[4]{\frac{\sigma P_T G^2 \lambda^2}{(4\pi)^3 k_b T_s \beta}} \tag{2.7}$$

On the perimeter security radar, the target is usually human, vehicle, animal, and so on. Therefore, the radar should be capable of detecting human and other potential threats. Since x-band radar is used in my laboratory measurements, table 3 below presents the RCS values of point-like targets in the x-band for perimeter security radars [16].

Targets	RCS [m2]	RCS [dB]
bird	0.01	-20
man	1	0
cabin cruiser	10	10
automobile	100	20
truck	200	23
corner reflector	20379	43.1

Table 2.1 RCS for Typical Targets at X-band [16]

The classification of radars, according to the waveform, can be seen in figure 2.3 below. The radar sensor used in this thesis is called X-band since it has a transmit frequency of 10.525 GHz. IEEE Standard Letter Designations for Radar Bands Used by the EESS Community and Their Comparison to the ITU (International Telecommunication Union) Allocations are presented in appendix A.

Since the HB100 sensor operating in X-band is a continuous wave doppler radar, the CW radar will be explained first. Then FMCW radar and signal processing theory, which is the main scope of the thesis, will be detailed. As mentioned earlier, the main focus of the thesis is to run the doppler radar in the FMCW form; the FMCW theory will be explained in detail.

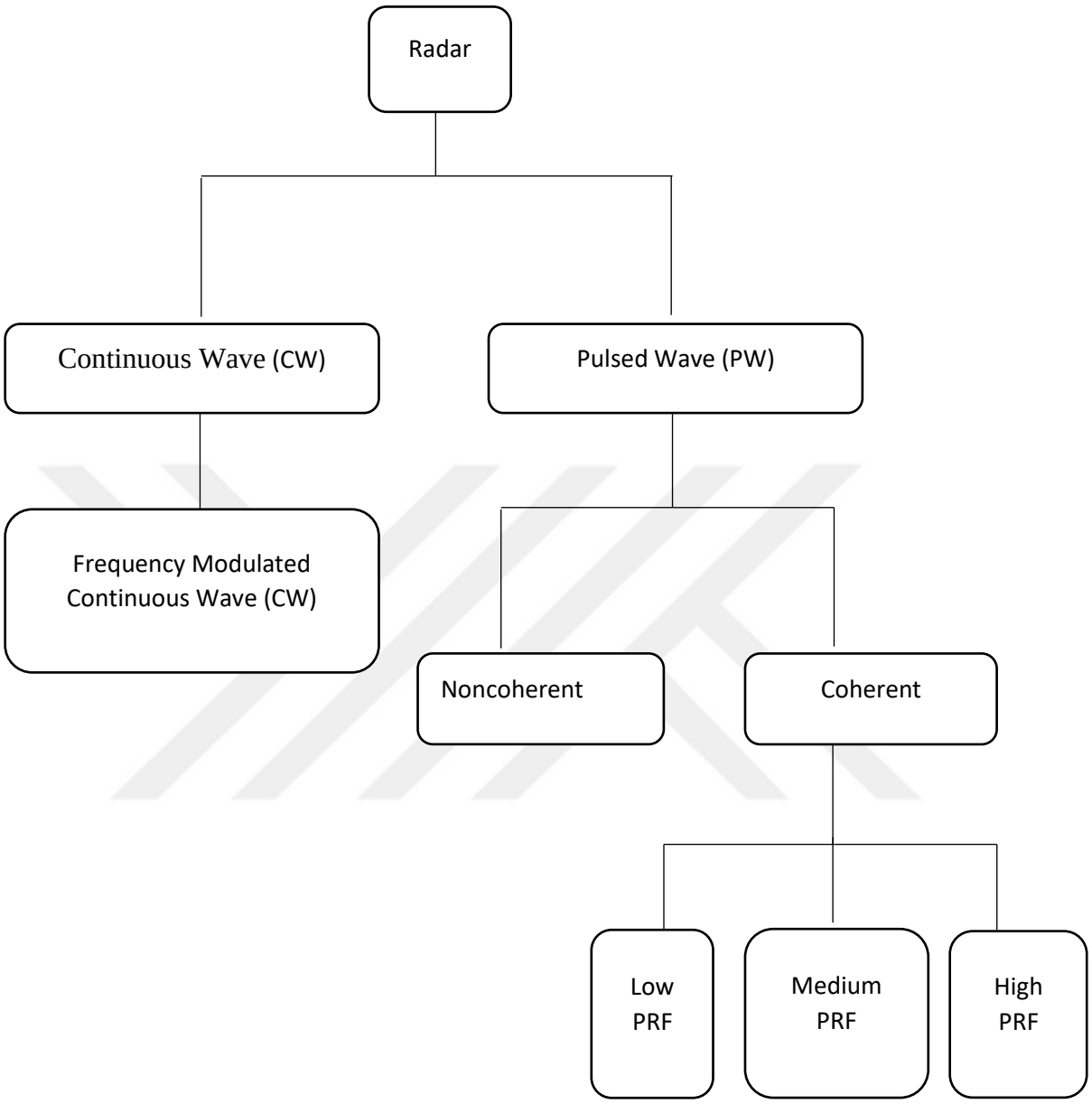


Figure 2.3 Classification of Radar System by Waveform [17]

2.2 Theory of CW Radar

Continuous-Wave (CW) radars transmit signals and receive the reflected signal from the target in an operating frequency. CW radars are based on the Doppler effect that changes the frequency of waves by moving the target relatively to the transmitter. Using the Doppler signal, the speed of the target can be calculated, but the distance of the target cannot be determined. The structure of the CW radar is presented in figure 2.4.[13] RF is generated in the oscillator, and it is transmitted by the transmitter antenna. The reflected signal is received by the receiver antenna, and then transmitted and received signals are given to the I/Q demodulator. The modulator mixes the transmitted and received signals by mixing shifted by 90 degrees transmitted wave and received wave. Signals from the I/Q demodulator are amplified and given to Analog to Digital Converters (ADC). The signal is now available for the application of different signal processing algorithms on the ADC output.

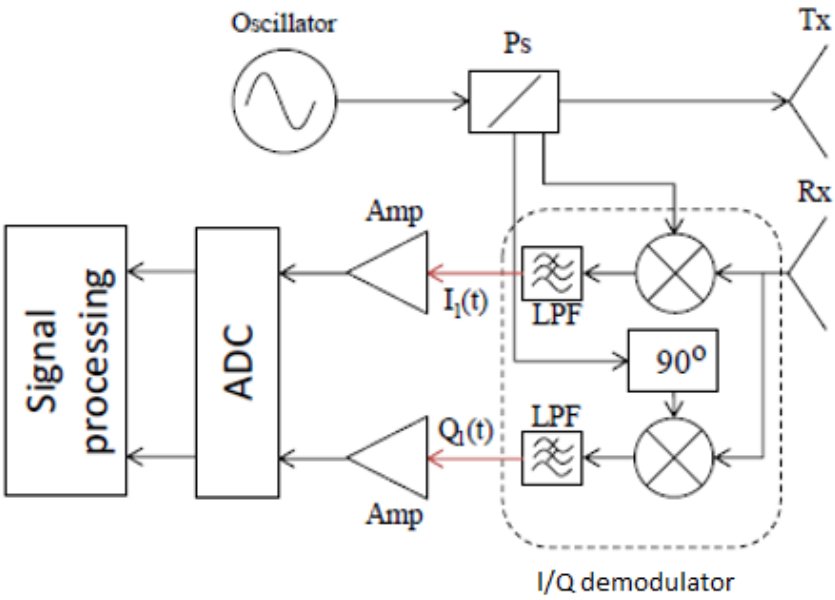


Figure 2.4 Structure of CW Radar Systems

Since the sensor used in the thesis is essentially a doppler radar sensor, the doppler radar is described in detail in the CW radar subheading. In the Perimeter Intrusion Radar Systems, it is necessary to explain the Doppler effect since the target is usually not stationary.

2.2.1 Doppler Radar and Velocity Calculation

Doppler radar was discovered by Christian Doppler in 1842. In a radar system, if the observed object is not stationary, the frequency of the received signal will be shifted from the frequency of the transmitted signal, known as the doppler effect, which is illustrated in figure 5. If the object moves towards the radar, the frequency of the received signal will increase. Similarly, If the object moves away from the radar, the frequency of the received signal will decrease.

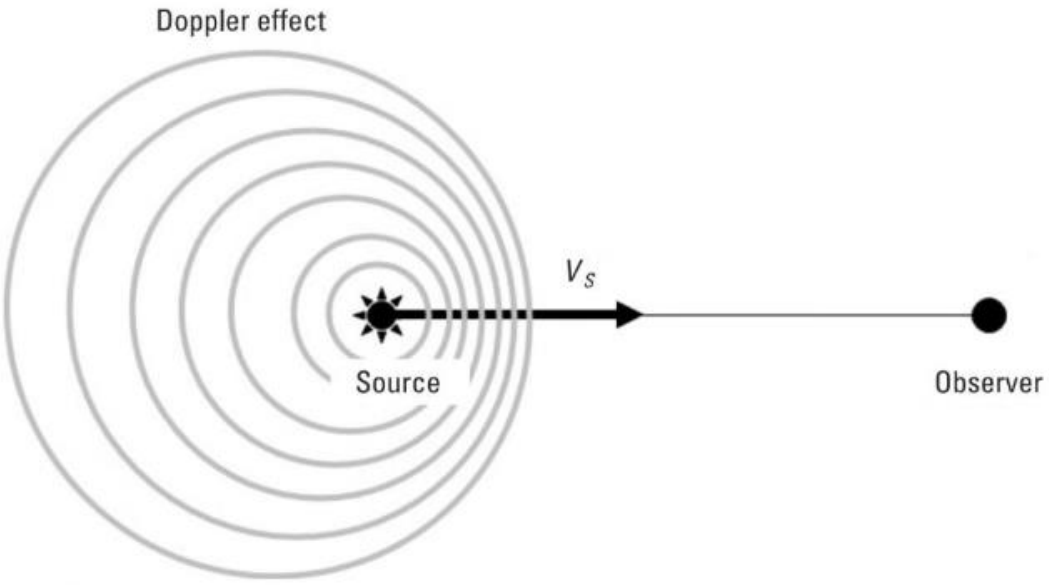


Figure 2.5 Doppler Effect [18]

The total distance between the radar and target is 2R because of the radar transmits a signal and receives an echo signal in a two-way communication path. The number of wavelengths (N_w), which are between the radar and target in 2R distance equal to equation 2.8.

$$N_w = \frac{2R}{\lambda} \tag{2.8}$$

where N_w is the total number of wavelengths, R is the distance between radar and target, λ is wavelengths. λ is corresponding to an angular excursion of 2π radians. Hence, the total angle

of excursion that caused by an electromagnetic wave along two-way communication between the radar and the target is equal to:

$$A_{exc} = \frac{4\pi R}{\lambda} \tag{2.9}$$

Angular frequency, ω is equal to:

$$\omega = 2\pi f \tag{2.10}$$

The relationship between angular frequency and phase angle is presented in equation 2.11.

$$\omega = \frac{d\phi}{dt} \tag{2.11}$$

where ϕ is the phase angle.

$$2\pi f = \frac{d\phi}{dt} \tag{2.18}$$

$$f = \frac{1}{2\pi}\frac{d\phi}{dt} \tag{2.19}$$

Since the total angle of the excursion is equal to ϕ and f is equal to doppler frequency (f_d).

$$f_d = \frac{1}{2\pi}\frac{d}{dt}\frac{4\pi R}{\lambda} \tag{2.110}$$

$$f_d = \frac{1}{2\pi}\frac{4\pi}{\lambda}\frac{dR}{dt} \tag{2.15}$$

$$f_d = \frac{2V_r}{\lambda} \tag{2.16}$$

Since λ is equal to the speed of light (c) over frequency (f), doppler frequency is presented in equation 2.17.

$$f_d = \frac{2V_r f}{c} \tag{2.17}$$

where f_d is the Doppler frequency, V_r is the relative velocity.

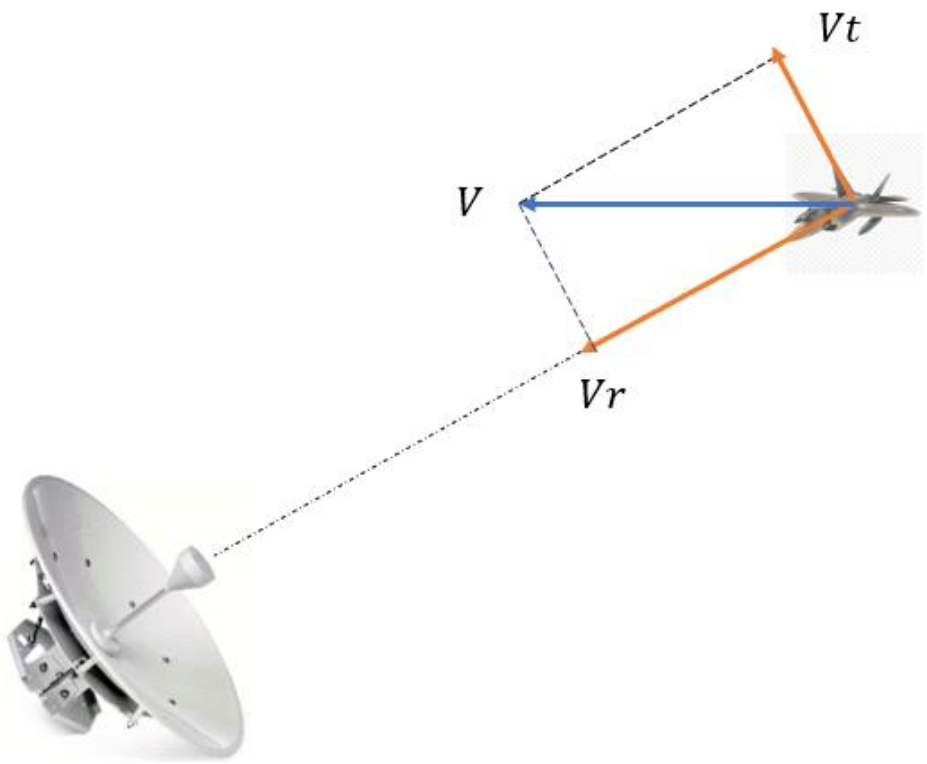


Figure 2.6 Radial velocity of moving target

2.3 Fundamentals of FMCW Radar

FMCW radars can calculate the range and speed of the target by taking advantage of frequency changes. For this reason, FMCW radars emerged by modulating and developing the CW waveform. A sawtooth, triangular, and sinusoidal signal can be used for modulation, and the signal that is obtained from modulation is called a chirp signal, which is a sinusoidal signal, as presented in figure 5. It is modulated to calculate the speed and range of the target at the same

time. The important parameters of the frequency-time representation of the chirp signal are start frequency (f_c), bandwidth (β), chirp duration (T_c), and Slope (S), as seen in figure 2.8-b. The slope can be calculated as given in equation 2.18.[21,22,24]

$$S = \frac{\beta}{T_c} \tag{2.18}$$

The general block diagram of the FMCW radars is presented in figure 1. The signal generator generates a chirp signal that will be divided into two different signals to obtain a local oscillator input signal for the mixer to be mixed with the received signal. The signal which is received by the antenna has a different frequency, phase, and power due to the target movement. The mixer that receives transmitter and receiver signals as input creates an Intermediate Frequency (IF) at its output [15,16, 25].

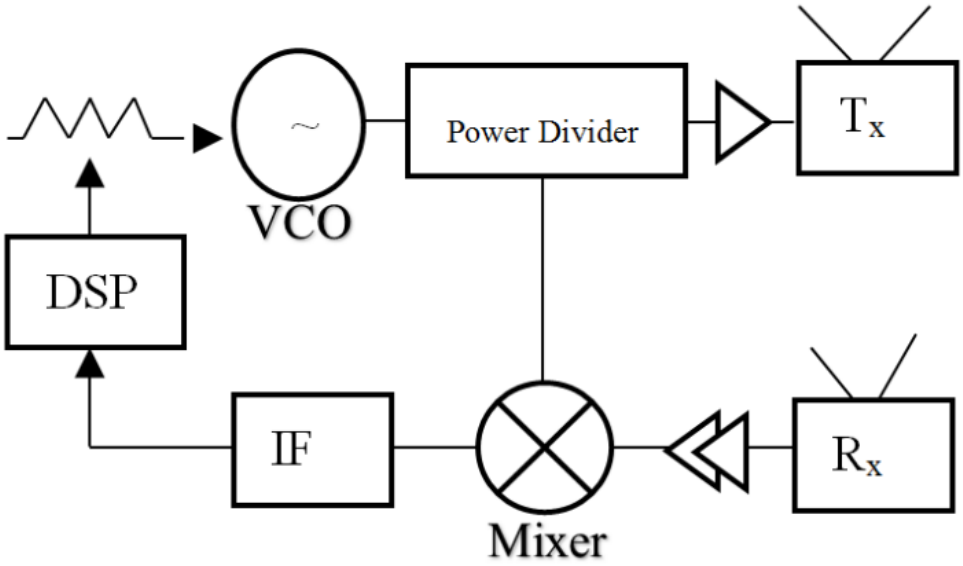
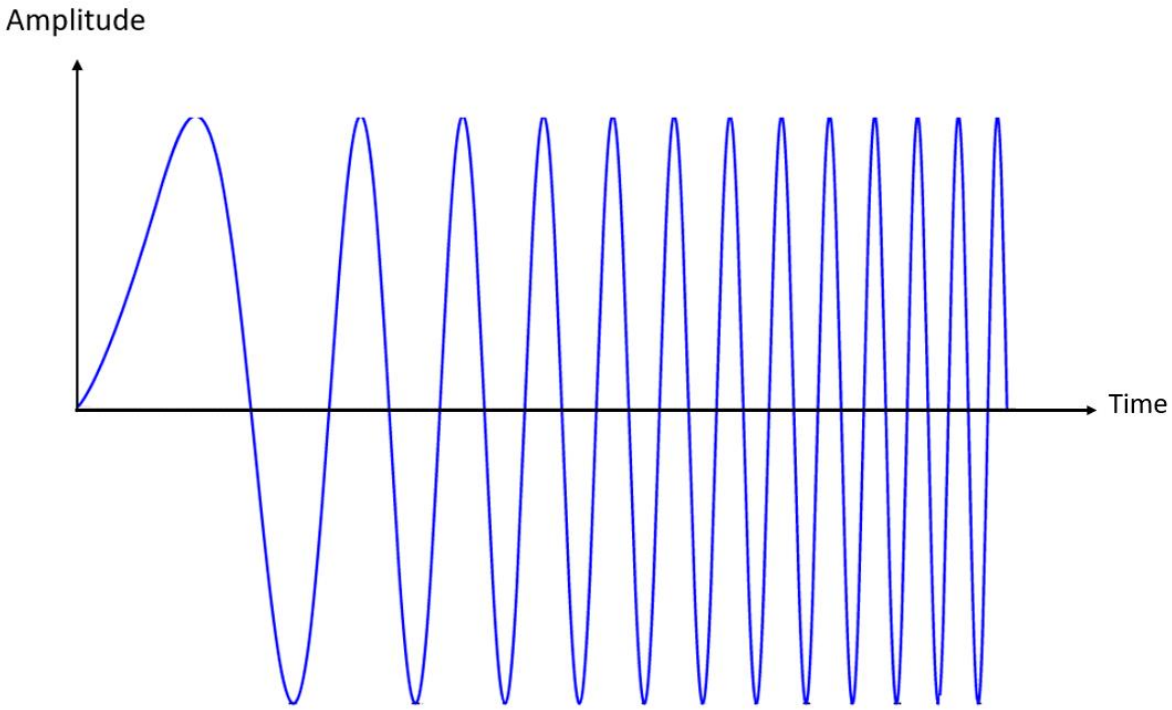
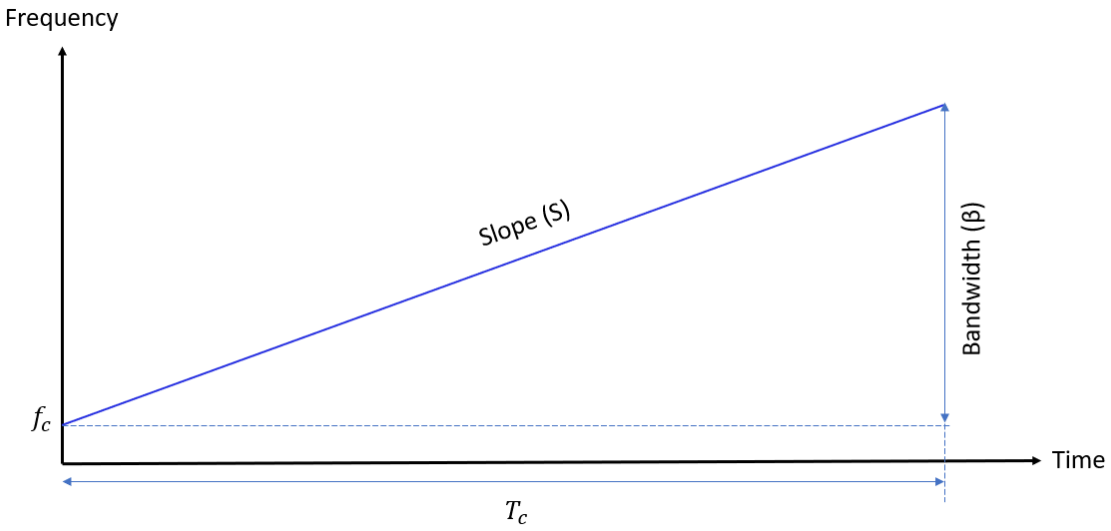


Figure 2.7 Block Diagram of FMCW Radar



(a)



(b)

Figure 2.8 (a) A sinusoidal chirp signal, and **(b)** frequency vs. time representation of chirp signal

In FMCW radar, range information can be obtained by the frequency offset between the transmitted and received signal. As shown in figure 2.9, the IF signal is the output of the mixer, where the transmitted and received signals are down-converted.

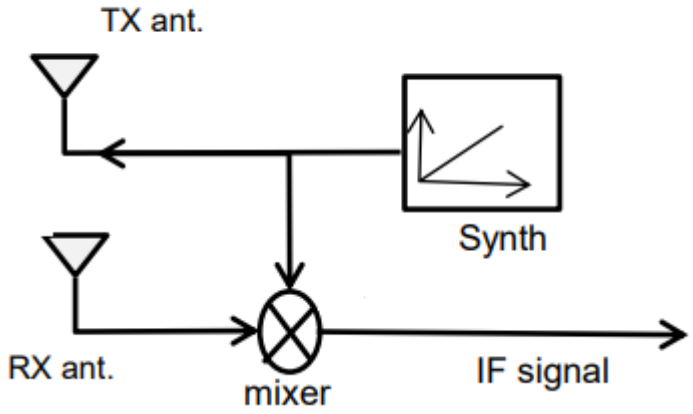


Figure 2.9 Working Principle of Mixer

A synthesizer (synth) generates a chirp, and then a chirp signal is transmitted by the T_X antenna. The chirp signal is reflected from an object, and the reflected chirp signal is received by the R_X antenna. The R_X signal and T_X signal are mixed, and the resulting signal is called an 'IF signal' as given in equation 2.21.

$$x_1 = \sin[\omega_1 t + \phi_1] \tag{2.19}$$

$$x_2 = \sin[\omega_2 t + \phi_2] \tag{2.20}$$

$$IF = x_1 - x_2 = \sin(\omega_1 - \omega_2)\, t + (\phi_1 - \phi_2) \tag{2.21}$$

where, ω_1 and ω_2 are instantaneous frequency of the two-input signal. ϕ_1 and ϕ_2 are the phase of the two input sinusoids. As mentioned earlier, the frequency of the signal that the output of the mixer is the difference of the instantaneous frequency of the TX-chirp and RX-chirp signals. If there is only one target in front of the radar, the IF signal has a constant frequency, as shown in figure 2.10.

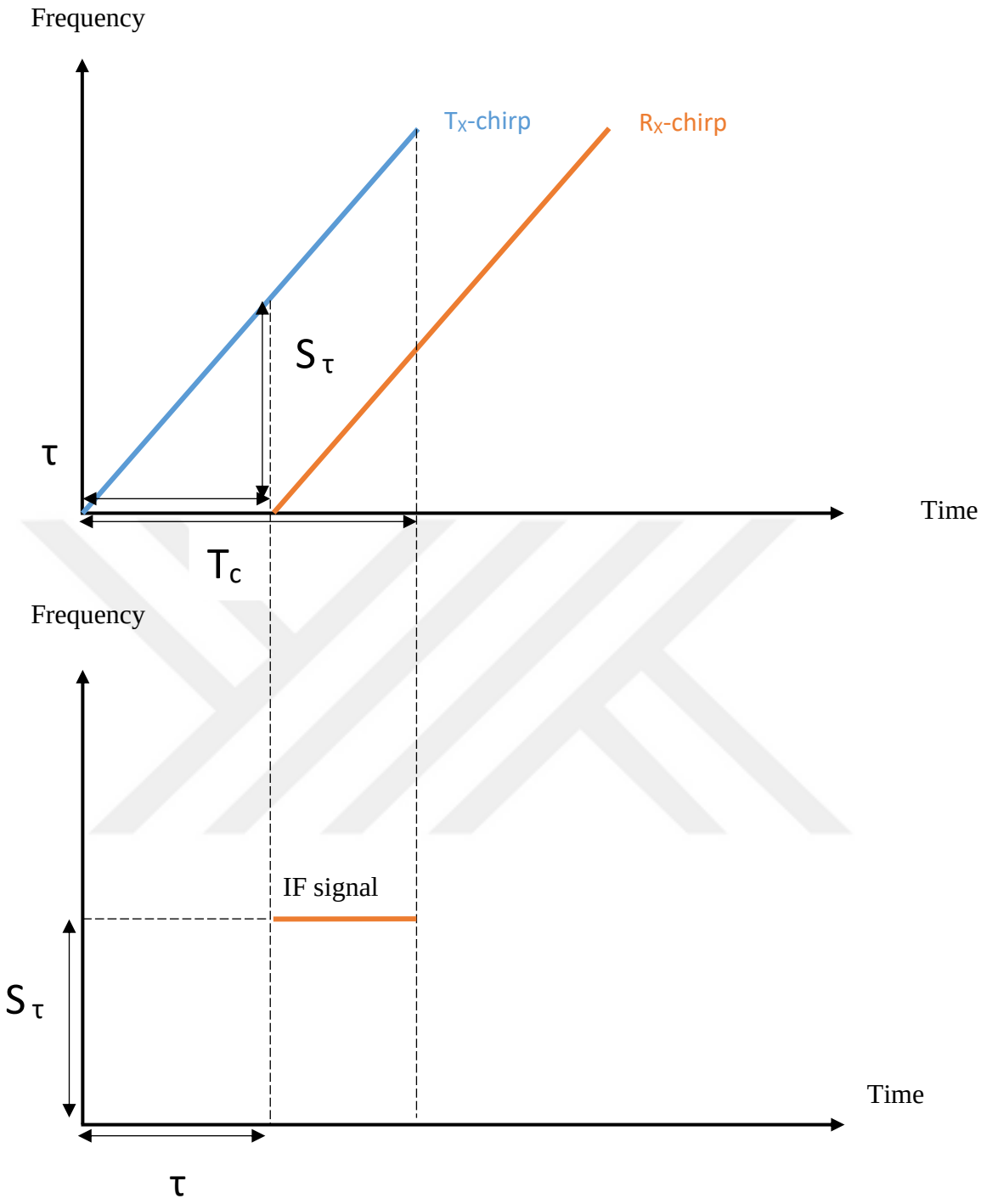


Figure 2.10 Transmitted and received signals and corresponding IF signal when a single object is in front of the antenna. [22,24]

The IF frequency can be calculated by using equation 2.32. The reflected echo signal would reflect by a target at the range R. The small fraction of the total chirp between the reflected and the transmitted signals are calculated by

$$\tau = \frac{2R}{c} \tag{2.22}$$

where is c (3x108 m/s) is the speed of light, and R is the range from target to radar. IF signal can be calculated by equation 2.23.

$$f_{IF} = S\tau \tag{2.23}$$

Equation 2.24 is obtained from equations 2.22 and 2.23.

$$f_{IF} = S\frac{2R}{c} \tag{2.24}$$

When the received and the transmitted signals are multiplied by the mixer, the beat frequency (f_b) can be extracted by filtering the high-frequency output signal. If the target is stationary, there is no Doppler effect in the signal, and f_b is expressed by the range of the target. If a sawtooth frequency-modulated waveform is used as in Figure 2.11, the resulting beat frequency will be constant except the reflection region.

$$f_b = |f_{Tx} - f_{Rx}| \tag{2.25}$$

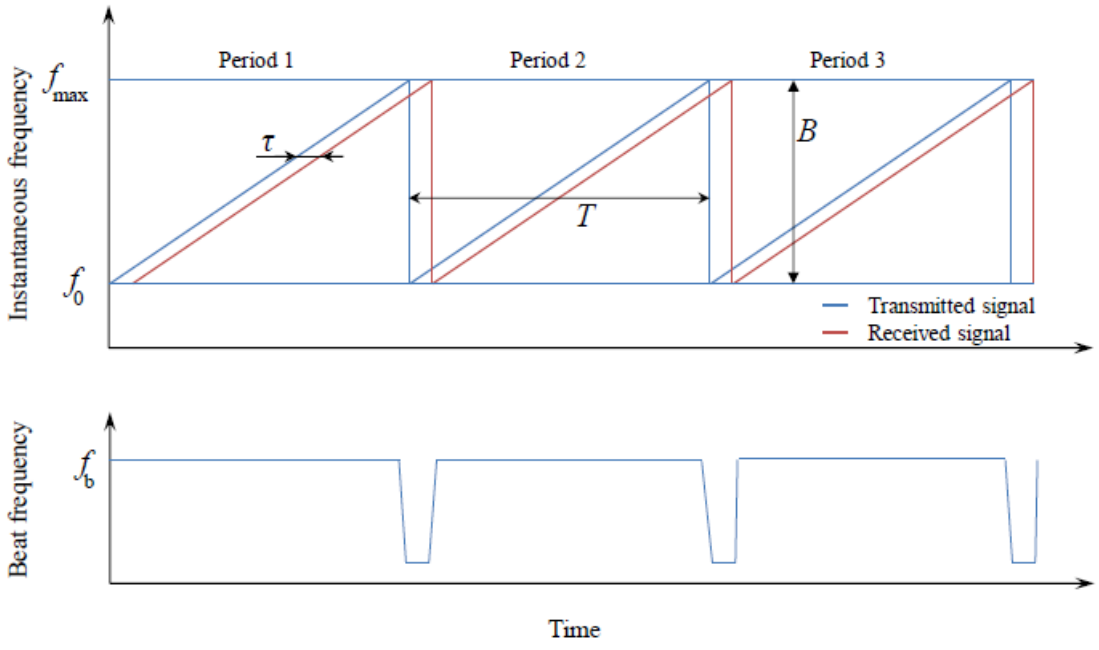


Figure 2.11 (Top) Instantaneous frequency of transmitted and received waves in case of a single stationary object. (Bottom) Resulting beat frequency. [23]

In the above equation f_b is the beat frequency, f_{Tx} is the transmit frequency and f_{Rx} is the receiver frequency. If the target is motionless, the following equation is achieved.

$$f_b = \frac{2\beta\tau}{T_c} \tag{2.26}$$

β refers to bandwidth, and Tm represents the triangular signal period.

From equation 2.23 and 2.27, the following equations were obtained.

$$f_b = \frac{2\beta R}{T_c c} \tag{2.27}$$

$$R = \frac{c f_b T_c}{2\beta} \tag{2.28}$$

The above equation can be used in case the target is stationary. The above equation can be used in case the target is stationary. However, In perimeter intrusion radar, generally, the target is not stationary. For a moving target, to calculate the range and velocity of the target at the scene, one can use triangular modulation, which results in two-beat signals with frequencies:

$$f_{bu} = f_b - f_d \tag{2.29}$$

$$f_{bd} = f_b + f_d \tag{2.30}$$

$$f_b = \frac{f_{bu} + f_{bd}}{2} \tag{2.31}$$

$$f_d = \frac{f_{bd} - f_{bu}}{2} \tag{2.32}$$

Figure 2.12 shows the behavior of instantaneous frequencies and beat frequency for triangular wave modulation.

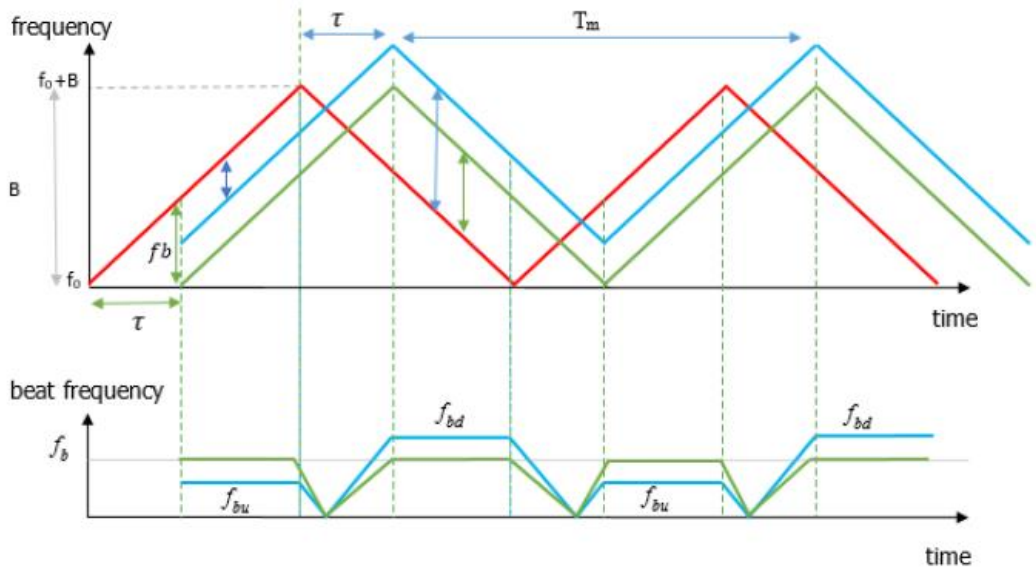


Figure 2.12 Transmitted, two received signals (modulation frequency) and two beat frequencies according to received signals.

where f_d is Doppler frequency, f_{bu} and f_{bd} are the beat frequency a

$$R = \frac{c(f_{bu} + f_{bd})T_m}{8\beta} \tag{2.33}$$

$$V_r = c(f_{bd} - f_{bu})4f_c \tag{2.34}$$

where R is the range, f_c is the center frequency of the transmitted signal, V_r is the relative speed of the target.

CHAPTER 3

EXPERIMENTAL SETUP

3.1 HB-100 Sensor

3.1.1 General Description

HB100 Miniature Microwave Motion Sensor is an X-Band Bi-Static Doppler transceiver module from the Agilsense Company [19], as shown in figure 3.1. The radar module consists of Dielectric Resonator Oscillator (DRO), microwave mixer, and patch antenna. Figure 3.2 shows a simplified block diagram of the HB100 sensor.



Figure 3.1 HB-100 Doppler Sensor Module

This sensor is generally used as a motion sensor. It is used in applications such as motion detection, light control, and vehicle speed measurement. In this thesis, as mentioned earlier, the HB100 sensor, generally used as a doppler radar sensor, is aimed to be used as an FMCW radar. In this section, it is explained in detail how to use the HB100 sensor as FMCW radar. Besides, the antenna characteristics and some important parameters of the sensor are explained.

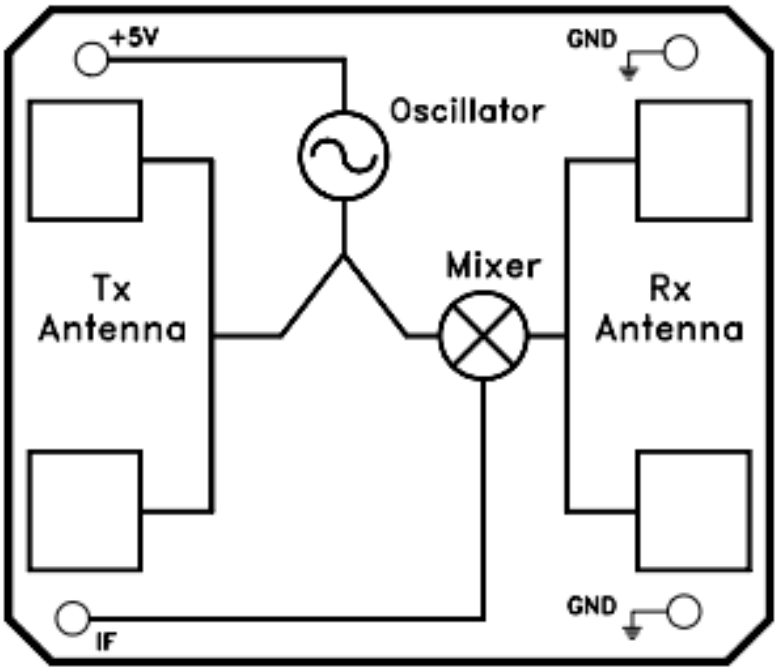


Figure 3.2 HB-100 Doppler Radar Block Diagram

The internal structure of the HB100 sensor is presented in figure 3.3.

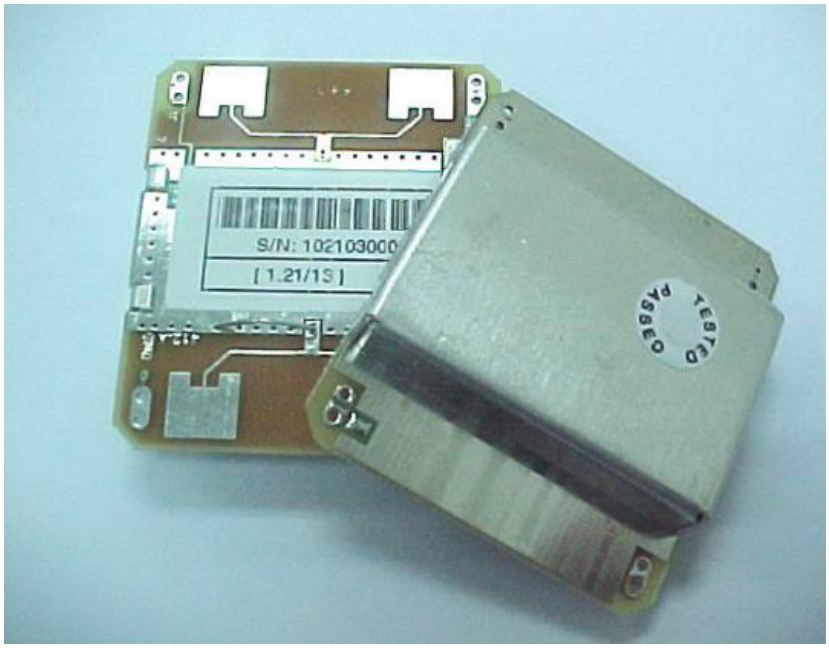


Figure 3.3 Internal Structure of the HB100 Sensor

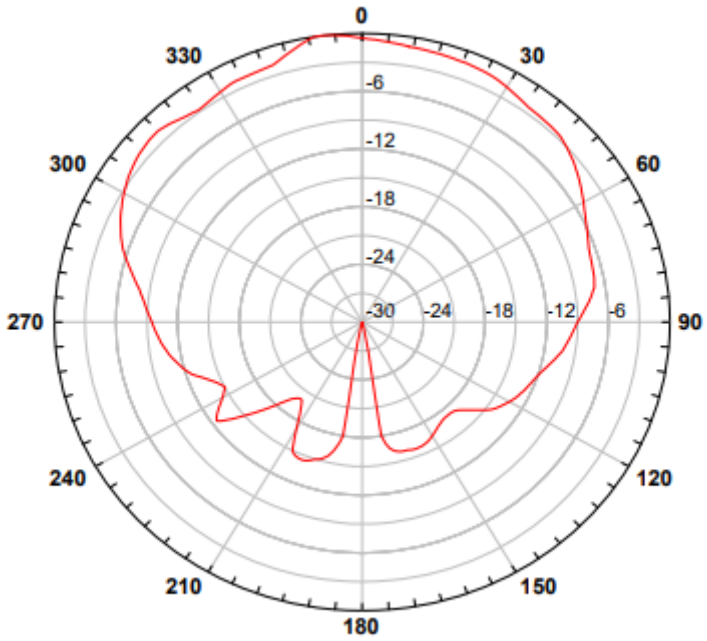
The important parameters of the sensor are presented in Table 3.1.

Parameter	Min	Typ.	Max	Units
Frequency Setting	10.520	10.525	10.530	GHz
Radiated Power (EIRP)	12	15	20	dBm
Spurious Emission			-7.3	dBm
Settling Time		3	6	µSec
Received Signal Strength		200		µVp-p
Noise			5	µVrms
Antenna Beam-width (3 dB) – Azimuth		72		°
Antenna Beam-width (3 dB) - Elevation		36		°
Supply Voltage	4.75	5.00	5.25	VDC
Current Consumption		30	40	mA
Pulse Repetition Frequency		2		KHz
Pulse Width	10			µSec
Operating Temperature	-15		55	°C
Weight		8		Gm

Table 3.1 Sensor Specifications

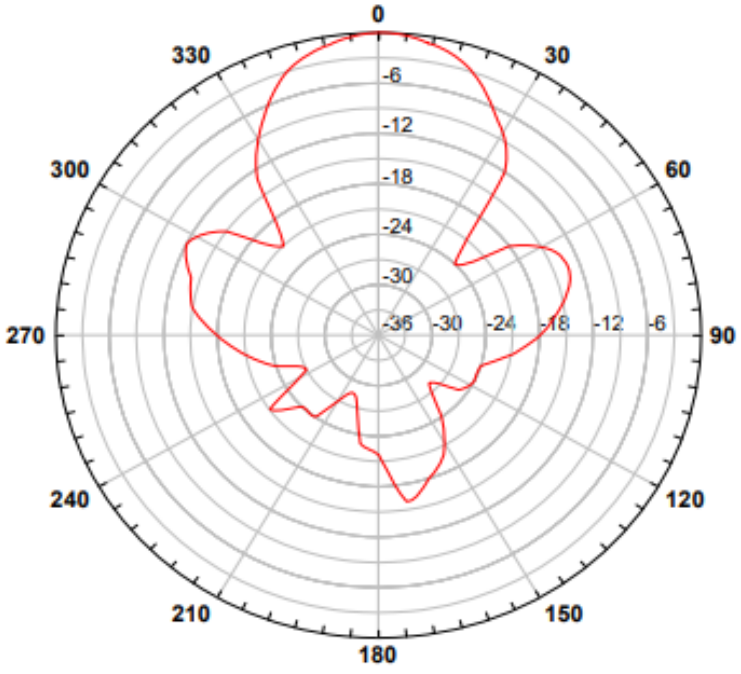
3.1.2 Antenna Specifications

As seen in figures 3.2 and 3.3, the sensor has an internal receiver and transmitter antenna. The azimuth and elevation beamwidth values of the antennas are 72 and 36 degrees, respectively. Relative to horizontal and vertical axes, the radiation patterns of the antenna are presented in figure 3.4. According to the figure, the antenna has low directionality values.



Azimuth

(a)



Elevation

(b)

Figure 3.4 Antenna Beam Pattern of HB-100 Sensor

Since the HB100 sensor, which mainly functions as a doppler radar, will be used as the FMCW radar, the sensor's features have been studied in detail. In this context, attention was paid to the features of the internal antennas of the sensor. Since it is tried to obtain distance information from the sensor, antenna parameters should be known in order to be used in calculations. The Equivalent Isotropic Radiated Power (EIRP) pattern of the HB-100 sensor was measured by Antenna Test Lab Company, and measurement results were shared. The image shared by the company regarding the HB-100 sensor tests is presented in figure 3.5.

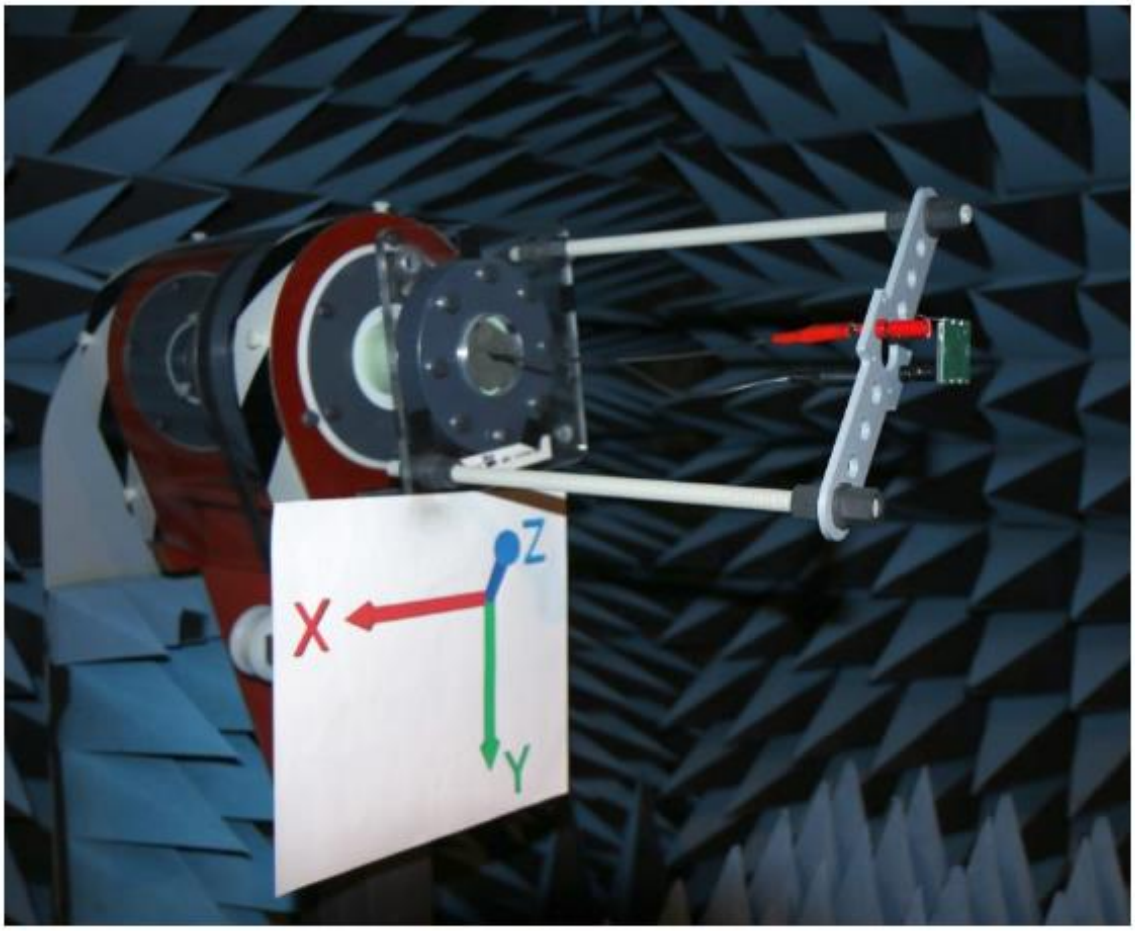


Figure 3.5 HB-100 sensor test [23]

The image obtained by drawing the EIRP values shared by the company with the 3D Plotting Spherical Software [26] of the company is presented in figure 3.6

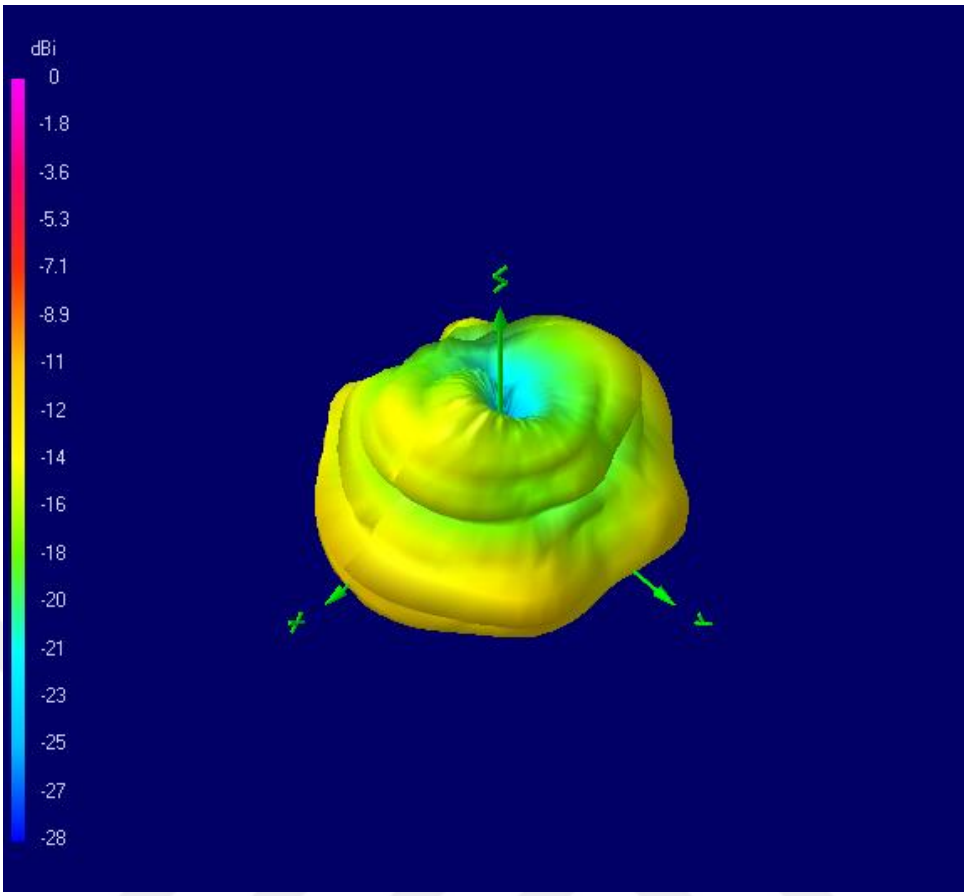


Figure 3.6 HB-100 sensor measured EIRP Pattern

3.1.3 Use of HB100 Sensor as FMCW radar

So far, the general characteristics of the sensor and antenna specification have been explained in the previous subtitles. In this section, it is described how the HB100 radar sensor is used as an FMCW radar.

Although the HB-100 sensor is known to be the doppler radar motion sensor, when the 5-Volt input supply voltage of the sensor was modulated with a triangular wave, a 3 MHz difference in output frequency between 10525 - 10528 MHz was detected, which means that the sensor can be used as an FMCW radar and the distance information of the stationary target can be obtained. The difference of 3 MHz refers to the bandwidth of the system. Therefore, Δf will be 3 MHz in the calculations to be made in the next chapter. Also, the sweep frequency of the system is determined as 10 kHz. All parameters which are given according to the sensor characteristics are presented in table 3.2.

Parameter	Typ.	Units
Frequency Setting	10.525	GHz
Transmitted Power Output	13	dBm
Receiver Sensitivity	-86	dBm
$\Delta f = \mathrm{B}$	3	MHz
Sweep Frequency	10	kHz
Sweep Rate	2	kHz
Receiver Antenna Gain	8	dBi
Receiver Beamwidth (Vertical)	36	°
Receiver Beamwidth (Horizontal)	72	°

Table 3.2 Sensor parameters to be used in FMCW radar calculations

Detailed explanation and calculations regarding the use of the sensor as FMCW radar will be made in the next chapter.

3.2 Lens Design

When the sensor's internal antennas are used, the range is less than 150 meters. For this reason, in order to increase the range, the lens, which is specifications given below, was designed in ZEMAX optical system design program. The designed and produced lens is shown in figure 3.7.

3.2.1 Lens Specification

The designed lens parameters are presented below.

- 20 cm Diameter,
- 16.9 cm Spherical Radius,
- 0.61 conic High-Density Polyethylene (HDPE),
- 1.6 Refractive Index .

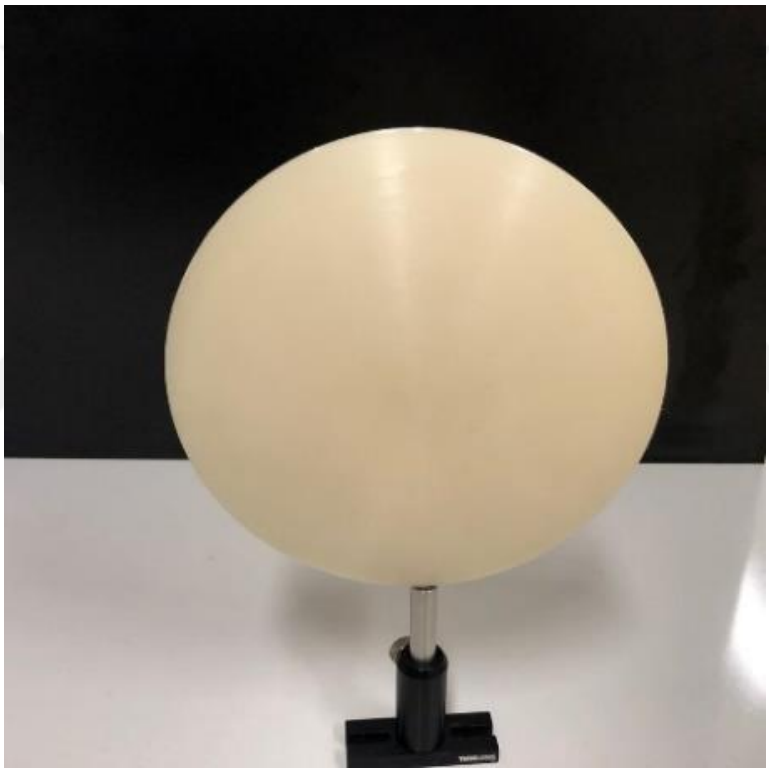


Figure 3.7 Designed Lens for Antennas

The beam spot diagram of the lens, drawn with the geometric optic assumption at 1 km away, is shown in figure 3.8. In addition, the beam lens radiation pattern image of the designed lens is shown in figure 3.9.

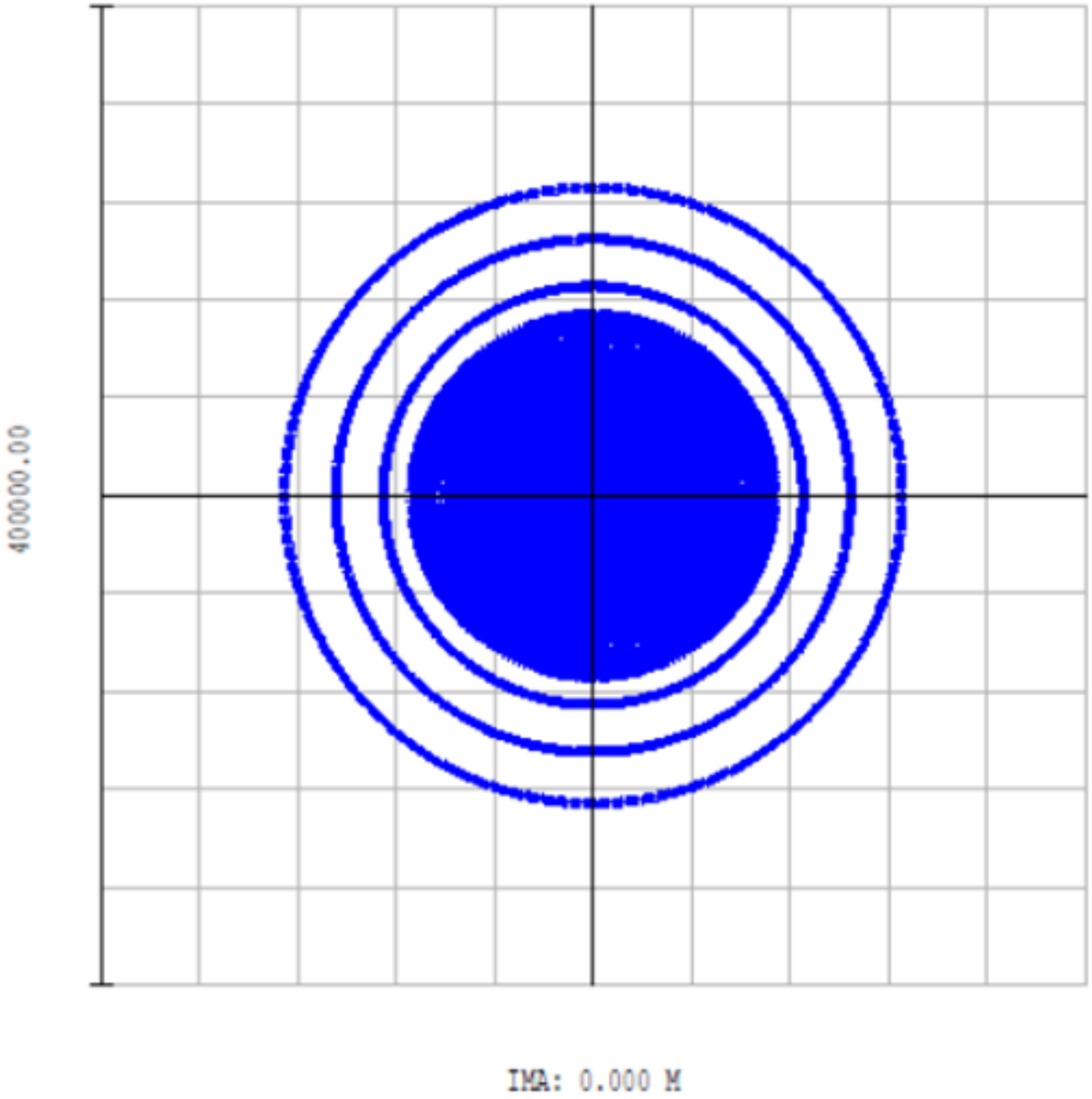


Figure 3.8 Beam Spot Diagram

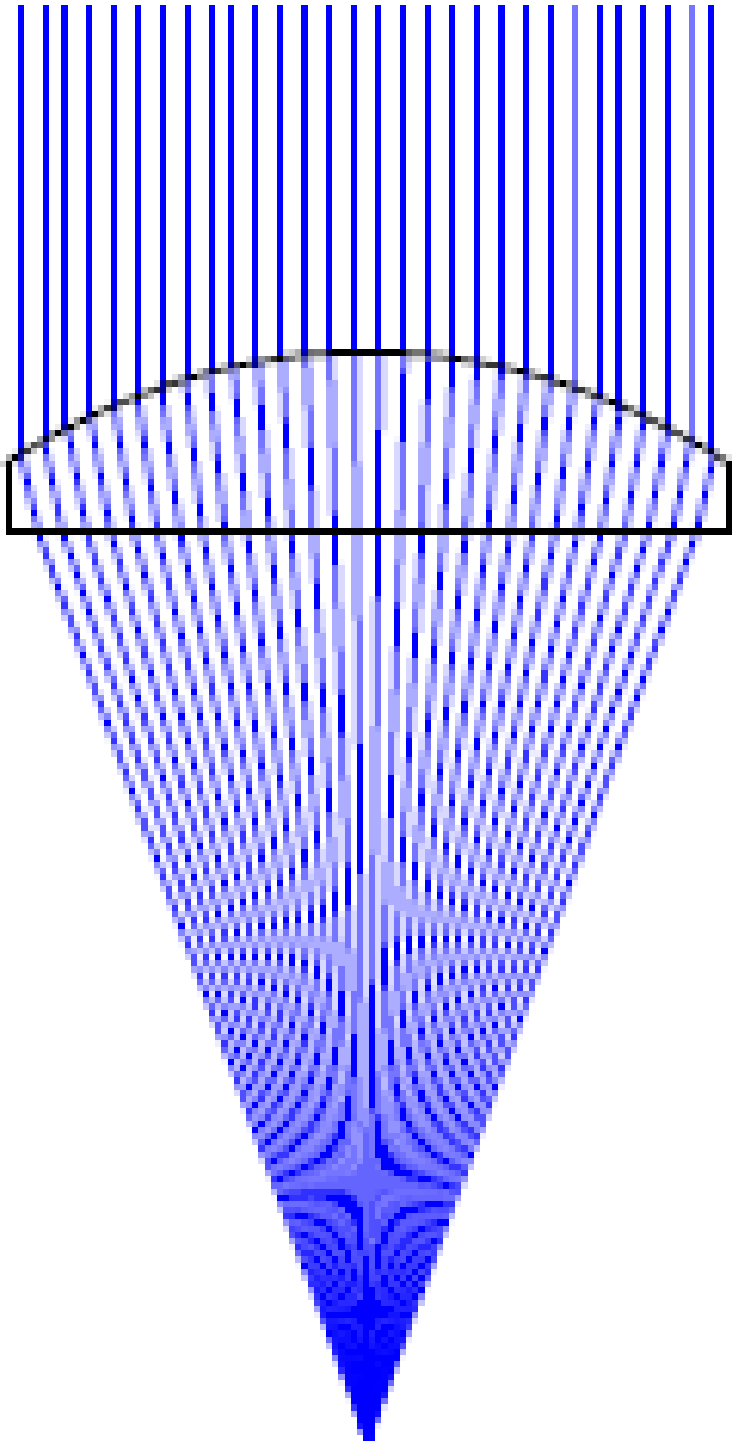


Figure 3.9 Beam Lens Radiation Pattern

As seen in Table 3.2, the sensor's internal receiver antenna horizontal and vertical beamwidth values are 36 and 72 degrees, respectively. Since these beamwidth values are not sufficient for target detection from a long distance, an external dielectric lens has been designed in order to

detect targets from longer distances by increasing the antenna gain, which is calculated by equation 3.1.

$$\mathrm{G} = \frac{4\pi}{\theta_h . \theta_v} \tag{3.1}$$

where G is the antenna gain, θ_h and θ_v are the horizontal and vertical beamwidth of the antenna in radians units, respectively. If the beamwidth values are substituted in equation 3.1, the antenna gain is calculated as 12 dB.

The external lens has been designed to increase the antenna gain, thus increasing the target detection range. According to the "conservation of étendue" theory, which is used for this purpose, the narrow-diameter and wide-angle beam were transformed into a wide-diameter and narrow-angle beam with the designed lens. According to the "conservation of étendue principle" detailed below, the product of beam diameter and beam spread angle must be constant. It is known that the diameter of the internal receiver of the sensor is 1 cm and the beam width is 36 and 72 degrees. If a 20 cm diameter lens is used, beamwidth values of 36 and 72 degrees are converted to 1.8 and 3.6 degrees by using equation 3.2.

$$D_{b1} . Bw_{a1} = D_{b2} . Bw_{a2} \tag{3.2}$$

where, D_{b1} and D_{b2} are the diameter of the internal antenna and diameter of the designed lens, respectively. Bw_{a1} and Bw_{a2} are beamwidths of the internal antenna and beamwidth of the system with the lens.

3.2.2 Conservation of étendue

Etendue is a geometric property of light that quantifies how to spread out the light spatially and angularly in an optical system. [27]. Etendue expresses the product of the area of the source, and the solid angle, which light emitted from that area subtends, mathematically. The etendue principle in two dimensions is visualized, as in figure 3.10, and it can be calculated by equation 3.3.

$$\epsilon = 2 . d . n . \sin(\theta) \tag{3.3}$$

where ϵ represents etendue, n is the index of refraction. The etendue in an optical system is conserved. According to the etendue principle, the minimum aperture width can be calculated in equation 3.4.

$$d_{ap} = d_s . \frac{n_s . \sin(\theta_s)}{n_{ap} . \sin(\theta_{ap})} \tag{3.4}$$

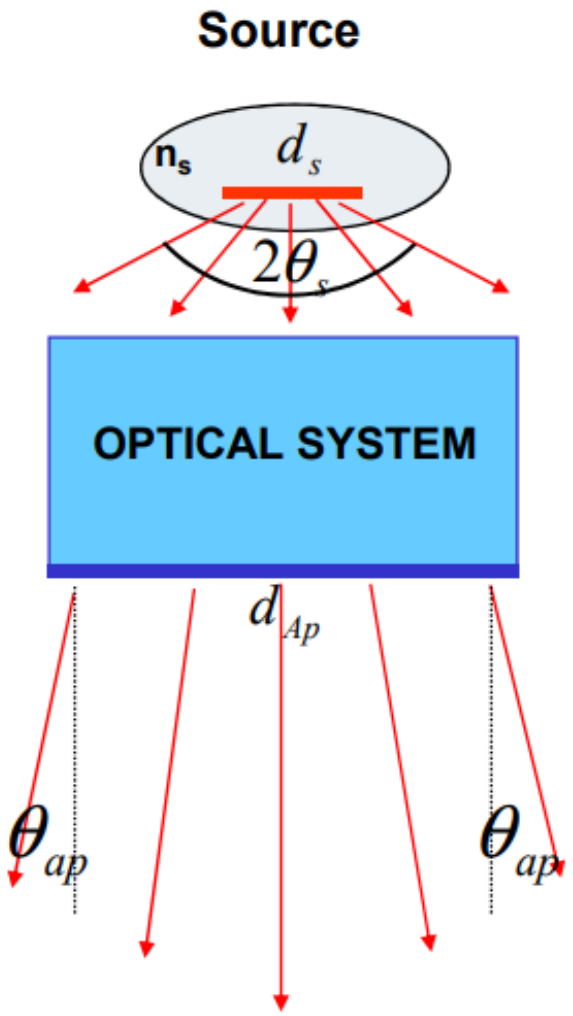


Figure 3.10 Visualization of etendue [28]

Etendue in 3D is shown in figure 3.11, and it can be calculated by equation 3.5. If the area of a light source increases, the etendue increases. Besides, as the solid angle decreases, the etendue decreases. And also, etendue has units of length squared.

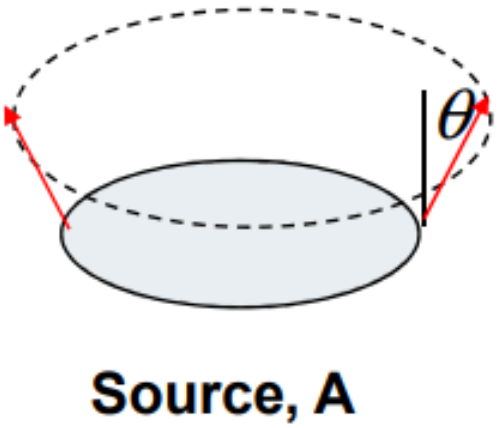


Figure 3.11 Simplified Visualization of 3D etendue [28]

$$\epsilon = \pi . n^2 . sin^2(\theta) . A \quad [L^2] \tag{3.5}$$

In the equation, ϵ is etendue, n represents the index of refraction, A is the area of source or pupil, θ is the cone angle of light cone emitting from source/pupil [27]. The advantageous and essential property of etendue is that it is conserved in a perfect optical system. As explained above, the antenna beamwidth is narrowed by designing an external lens with the etendue conservation principle. As a result, it has been explained that the target detection range can be increased with the designed lens. Using equation 3.2 described above, 36 degrees horizontal beamwidth was converted to 1.8 degrees, i.e., 31.4 milliradians. Similarly, the 72 degrees vertical beamwidth was converted to 3.6 degrees, i.e., 62.8 milliradians. When these values are substituted in equation 3.1, the antenna gain is calculated as 38 dB. The effect of antenna gain on the target detection range will be explained in detail in the next section.

3.3 Explanation of the General System

HB100 sensor and other subsystems are described above. The test measurement setup, including the HB-100 sensor and the designed lens prepared in the laboratory, is presented in below figure 3.10.

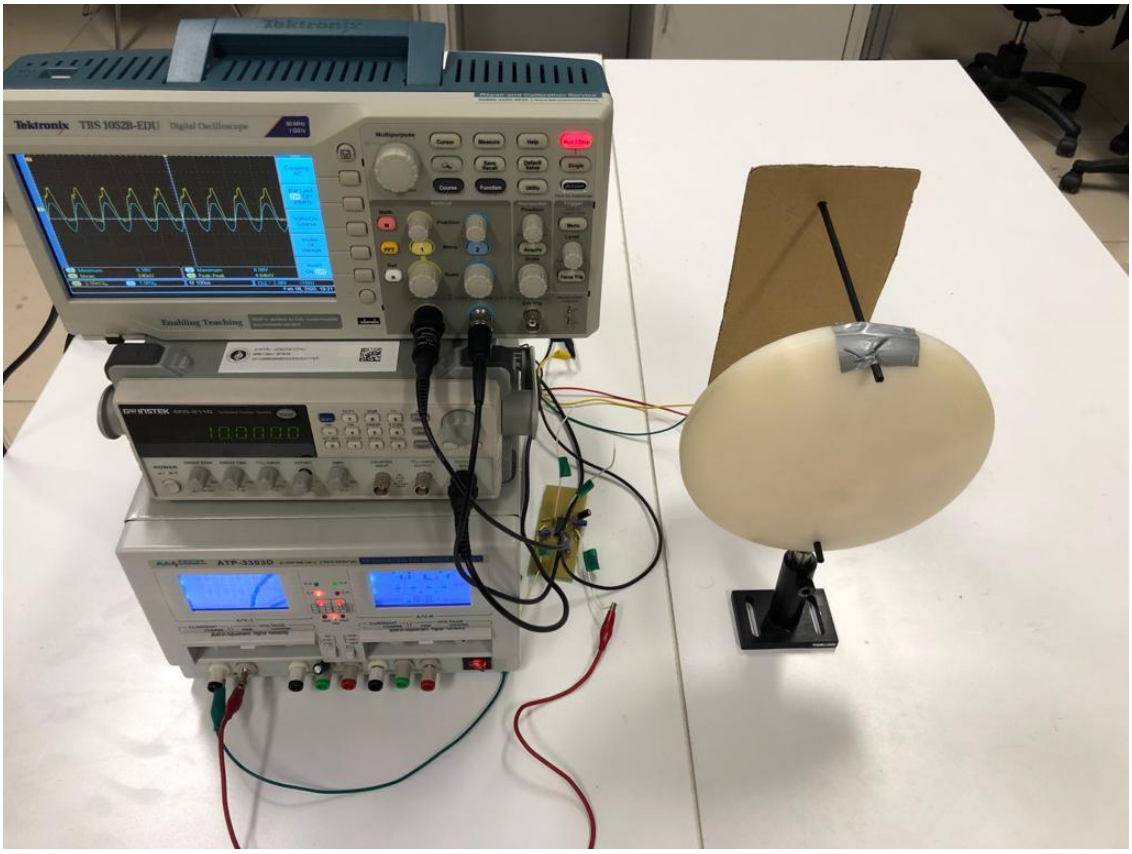


Figure 3.12 Test Setup

During the laboratory measurements, the HB100 sensor was operated with a 5 V symmetrical triangle wave. As a result, it was observed that a 3Mhz trace was formed on the spectrum analyzer.

CHAPTER 4

THEORETICAL CALCULATIONS

Before the theoretical calculations, the necessary system parameters were explained in detail in the previous chapters. In this context, HB100 sensor features, designed external lens parameters were introduced. In this chapter, the sensor parameters obtained by operating the simple doppler radar as FMCW radar will be explained in detail. Next, necessary concepts such as receiver sensitivity, minimum detectable signal, noise floor, noise figure will be introduced for maximum detection range calculation. Finally, using the internal receiver of the sensor and the externally designed lens, the maximum range will be calculated separately. Besides, beamwidth values calculated for both cases will be presented by visualization.

4.1 System Parameters for Maximum Detection Range Calculations

In this section, the necessary parameters for the calculation of the maximum target range of the sensor, which is operated as FMCW radar, will be reminded. Then, external lens parameters designed to increase antenna gain will be given.

4.1.1 HB100 Sensor Specification

Sensor parameters to be used in theoretical calculations are presented in table 4.1. Antenna parameters are excluded as they are explained in detail in the next section. Besides, the theoretical issues required for the max detection distance calculation will be described. Finally, maximum detection range calculations will be given for the system with and without lenses.

Parameter	**Typ.**	**Units**
Frequency Setting	10.525	GHz
Transmitted Power Output	13	dBm
Receiver Sensitivity	-86	dBm
$\Delta f = \beta$	3	MHz

Sweep Frequency	10	kHz
Sweep Rate	2	kHz

Table 4.1 HB100 Sensor Parameters

4.1.2 Antenna Parameters

The internal antenna and lens parameters of the sensor are explained in detail in section 3.1.2. In this section, the interior antenna characteristics, the antenna gain calculated for the external 20 cm diameter lens, and the 40 cm diameter lens are summarized in Table 4.2. Although the actual measurements were made with only a 20 cm diameter lens, I wanted to explain what the results would be if a 40 cm lens were used.

Parameters	**Without Lens**	**20 cm Diameter Lens**	**40 cm Diameter Lens**
$\theta_h\ (degrees)$	36	1.8	0.9
$\theta_v\ (degrees)$	72	3.6	1.8
$\theta_h\ (radians)$	0.6283	0.0314	0.0157
$\theta_v\ (radians)$	1.2566	0.0628	0.0314
$G(linear)$	15.92	6373	25491
$\boldsymbol{G(dB)}$	**12**	**38**	**44**

Table 4.2 Antenna Gain Calculation

In table 4.2 above, G represents the antenna gain, θ_h and θ_v are the horizontal and vertical beamwidth of the antenna, respectively. As explained earlier, the horizontal and vertical beamwidth values in lens systems were calculated according to the conservation of the étendue principle described in section 3.2.2 above.

4.2 FMCW Radar Maximum Detection Range Calculations

In radar equations, sensor characteristics such as Receiver Sensitivity, Noise Factor (NF), Minimum Detectable Signal (MDS) should be known in order to calculate the maximum target detection range. The receiver sensitivity of the HB100 sensor is known to be -86 dBm. In this sensor, the factor limiting the receiver sensitivity is the leakage, not the noise figure. Although the oscillator is assumed to be at a fixed frequency, even if the sensor is operated with constant DC, the phase noise of the HB100 sensor is high because the dielectric resistor is of low quality, and the feedback path is unprotected. Therefore, a low-frequency noise signal IF is formed with leakage and self downconversion in the mixer. 10 μVrms can be considered as noise. Besides, the SNR is specified as 10 dB in the sensor datasheet.

For FMCW radar systems, the $SNR_{compress}$ value can be calculated with equation 4.1 without integration. The maximum detection range can be obtained from this equation.

$$SNR_{compress} = \frac{P_t G_t G_r \lambda^2 \sigma}{(4\pi)^3 R^4 k T \beta F} B\tau \tag{4.1}$$

where:

P_t = Transmitted Power,

G_t = Transmit Antenna Gain,

G_r = Receive Antenna Gain,

λ = Wavelength of Radar Signal,

σ = Radar Cross Section (RCS),

k = Boltzmann's Constant (1.38×10^{-23} J/K),

T = Absolute Temperature of The Receiver Input (290 °K),

β = Receiver Bandwidth,

F = Noise Factor,

τ = Sweep Period.

Since the target was generally considered to be human in PIR, the RCS value was assumed to be 1 m^2. In addition, the surface reflectivity value for humans was taken as 0.1. All system parameters are presented in table 4.3 below.

Parameter	Value	Unit
P_t	13	dBm
G_t	12 or 38 or 44	dB
G_r	12 or 38 or 44	dB
λ	3	Cm
σ	1	m^2
k	$1.38x10^{-23}$	J/K
T	290	°K
β	3	MHz
F	10	dB
τ	0.5	ms

Table 4.3 System Parameters

Antenna gain values in the table vary depending on whether an external lens is used in the system. If an external lens is used, the antenna gain varies according to the diameter of the lens. In summary, if no lens is used in the system, the antenna gain is 12 dB. If a lens with a diameter of 20 cm is used in the design, the antenna gain is 38 dB, and if a 40 cm diameter lens is used, the antenna gain is calculated as 44 dB.

In equation 4.1, the $kT\beta F$ value in the denominator was accepted as -86 dBm, that is, the receiver sensitivity. In fact, as seen in equation 4.3, the result was expected to be -98 dBm, but because of leakage and phase noise, the $kT\beta F$ value was used directly as the receiver sensitivity.

$$kT\beta F\ (dB) = 10log_{10}(1.38.10^{-23}.290.1000) + 10log_{10}(3.10^{6}) + 10log_{10} \quad (4.2)$$

4.2.1 Calculation of Maximum Detection Range without Using an External Lens

When the external lens is not used, the antenna gain is 12 dB. If the antenna gain values are substituted in equation 4.1, equation 4.4 is obtained.

$$SNR_{compress}(dB) = 13 + 2.12 + 20log_{10}(3.10^{-2}) + 10log_{10}(0.1) + 10log_{10}(3.10^{-2}) - 30log_{10}(4\pi) - 40log_{10}(R) - (-86) \quad (4.3)$$

$$SNR_{compress}(dB) = 70.5 - 40log_{10}(R) \quad (4.4)$$

The value calculated by Equation 4.4 is the instantaneous SNR value. Assuming we make coherent data acquisition, the coherent integration gain can be calculated with equation 4.5.

$$G_c = \frac{T_o}{P_s} \quad (4.5)$$

where G_c is Coherent Integration Gain, T_o is Observation Time, P_s is Sweep Period. Observation time varies according to the target to be detected by radar. For PIR, we assume that the target is human on foot. Considering the target maximum speed of 10 m/s and the target area size of 1 meter, observation time is calculated as 0.1. It was previously stated that the sweep period value is 0.5 ms. T_o and P_s are substituted in the equation 4.5, Coherent Integration Gain value is calculated as 23 dB. For reliable detection with the current sensor, the SNR value is expected to be 10 dB, and equation 4.7 can be obtained.

$$SNR_{compress+coherent\ gain}(dB) = 70.5 - 40log_{10}(R) + 23 \quad (4.6)$$

$$70.5 - 40log_{10}(R) + 23 \geq 10 \quad (4.7)$$

$$122\ m \geq R \quad (4.8)$$

From Equation 4.7, the maximum range is 122 meters. If Coherent Integration Gain is not taken into account, from equation 4.9, the instantaneous maximum range value is calculated as 32.5 meters.

$$70.5 - 40log_{10}(R) \geq 10 \quad (4.9)$$

$$32.5\, m \geq R \quad (4.10)$$

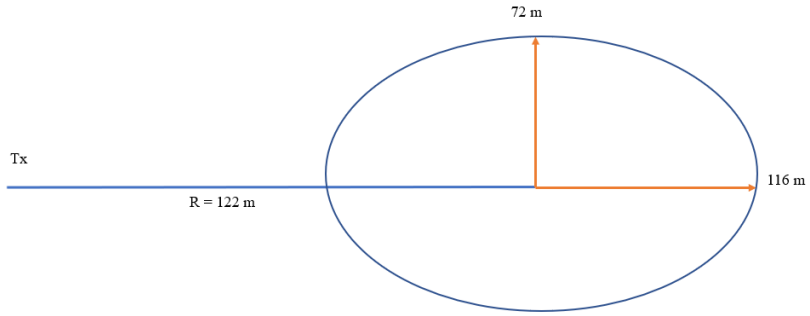
4.2.1.1 Beamwidth Calculation without Using External Lens

The maximum range was calculated when the external lens was not used. When Coherent Integration Gain is taken into account, it is calculated as 122 meters, and when not taking into account, it is calculated as 32.5 meters. According to the calculated max range values, beamwidth calculation can be done with the given equations 4.11 and 4.12.

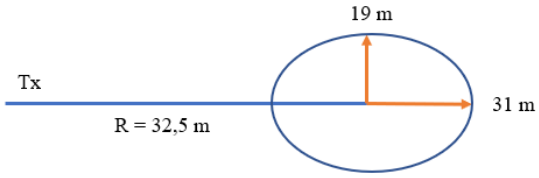
$$B_{wh} = R.\sin(\theta_h) \quad (4.11)$$

$$B_{wv} = R.\sin(\theta_v) \quad (4.12)$$

where R is a range, θ_h and θ_v are the horizontal and vertical beamwidth of the antenna, respectively. When the above equations are applied for 122 meters range, beamwidth values 72 and 116 meters are calculated. When the range is 32.5 meters, beamwidth values are found as 19 and 31 meters. The calculated beamwidth values are visualized in figure 4.1-a and 4.1-b.



(a)



(b)

Figure 4.1 (a) Beamwidth for 122 m **(b)** Beamwidth for 32,5 m

4.2.2 Calculation of Maximum Detection Range Using 20 cm Lens

In the case of using an external lens with a diameter of 20 cm, the antenna gain was calculated as 38 dB. The new $SNR_{compress+coherent\ gain}$ value is given in equation 4.13.

$$SNR_{compress+coherent\ gain}(dB) = 122.5 - 40log_{10}(R) + 23 \quad (4.13)$$

$SNR_{compress+coherent\ gain}$ value must be greater than or equal to 10 dB SNR value.

$$122.5 - 40log_{10}(R) + 23 \geq 10 \quad (4.14)$$

$$1440\ m \geq R \quad (4.15)$$

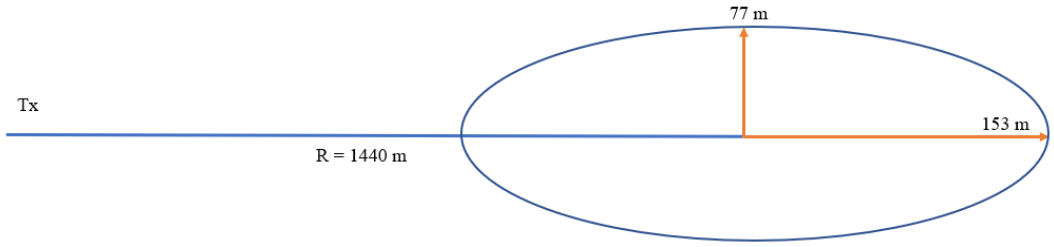
If Coherent Integration Gain is not taken into account, from equation 4.16, the instantaneous maximum range value is calculated as 650 meters.

$$122.5 - 40log_{10}(R) \geq 10 \quad (4.16)$$

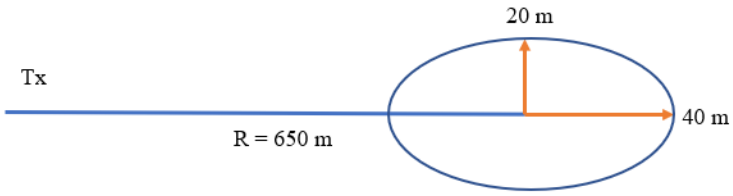
$$650\ m \geq R \quad (4.17)$$

4.2.2.1 Beamwidth Calculation Using 20 cm Lens

Beamwidth values calculated using the equations described in section 4.3.1.1 are 20 m x 40 m at 650 meters and 77m x 153 m at 1440 meters. Beamwidth values calculated with the same method were visualized in figure 4.2.



(a)



(b)

Figure 4.2 (a) Beamwidth for 1440 m **(b)** Beamwidth for 650 m

4.2.3 Calculation of Maximum Detection Range Using 40 cm Lens

Although the diameter of the lens used in the experimental setup was 20 cm, it was wanted to calculate how much the maximum detection distance would increase if a 40 cm lens were used. In the case of using a 40 cm diameter lens, the calculated antenna gain is 44 dB, as given in table 4.1. For the 40 cm diameter lens, $SNR_{\text{compress+coherent gain}}$ value is given in equation 4.18.

$$SNR_{compress+coherent\ gain}(dB) = 134.5 - 40log_{10}(R) + 23 \quad (4.18)$$

$SNR_{compress+coherent\ gain}$ value must be greater than or equal to 10 dB SNR value.

$$134.5 - 40log_{10}(R) + 23 \geq 10 \quad (4.19)$$

$$4870\ m \geq R \quad (4.20)$$

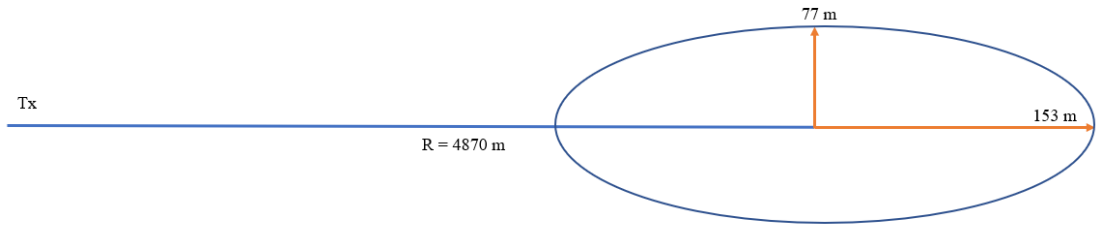
If Coherent Integration Gain is not taken into account, from equation 4.21, the instantaneous maximum range value is calculated as 1296 meters.

$$134.5 - 40log_{10}(R) \geq 10 \quad (4.21)$$

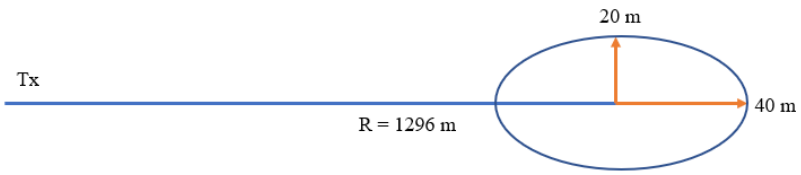
$$1296\ m \geq R \quad (4.17)$$

4.2.3.1 Beamwidth Calculation Using 40 cm Lens

Beamwidth values calculated using the equations described in section 4.3.1.1 are 20 m x 40 m at 1296 meters and 77m x 153 m at 4870 meters. Beamwidth values calculated with the same method were visualized in figure 4.3. As a result of the calculations, it was observed that the maximum distance increased as a result of doubling the lens diameter, but the beamwidth values did not change.



(a)



(b)

Figure 4.3 (a) Beamwidth for 4870 m **(b)** Beamwidth for1296 m

All calculated maximum range values and beamwidth values are presented in detail in table 4.4 below.

	Without Lens	20 cm Lens	40 cm Lens
Instantaneous Maximum Range (IMR)	32.5 m	650	1296
Maximum Range with Coherent Gain (MRCG)	122 m	1440	4870
Beamwidth (IMR)	19 x 31 m	20 x 40 m	20 x 40 m
Beamwidth (MRCG)	72 x 116 m	77 x 153 m	77 x 153 m

Table 4.4 Maximum Range and Beamwidth Values

4.2.4 Calculation of Range Accuracy

For FMCW radar, range accuracy is a variable value and depends on SNR. The higher the SNR, the smaller the range accuracy. The fundamental resolution is determined by equation 4.18.

$$S_r = \frac{\tau . c}{2} \tag{4.18}$$

where S_r is range resolution, τ is sweep period, 0.5 ms, and c is the speed of light (3.10^8 m/s). The resolution was calculated 75 km from the equation. However, with new signal processing techniques, this value can be reduced to sub-meter resolution[29,30]. In PIR, if more than one target is detected, the lowest resolution possible increases the radar performance rate.

CHAPTER 5

MEASUREMENT AND RESULTS

After the necessary designs were made, the relationship between IF and range was calculated and simulated by equation 4.1.

$$IF = 2.\Delta f.SweepFrequency.\tau \quad (5.1)$$

where Δf is the Bandwidth (BW), which is 3 Mhz for our designed setup. The sweep frequency of the system is 10 kHz, and τ is the propagation delay calculated by equation 2.23.

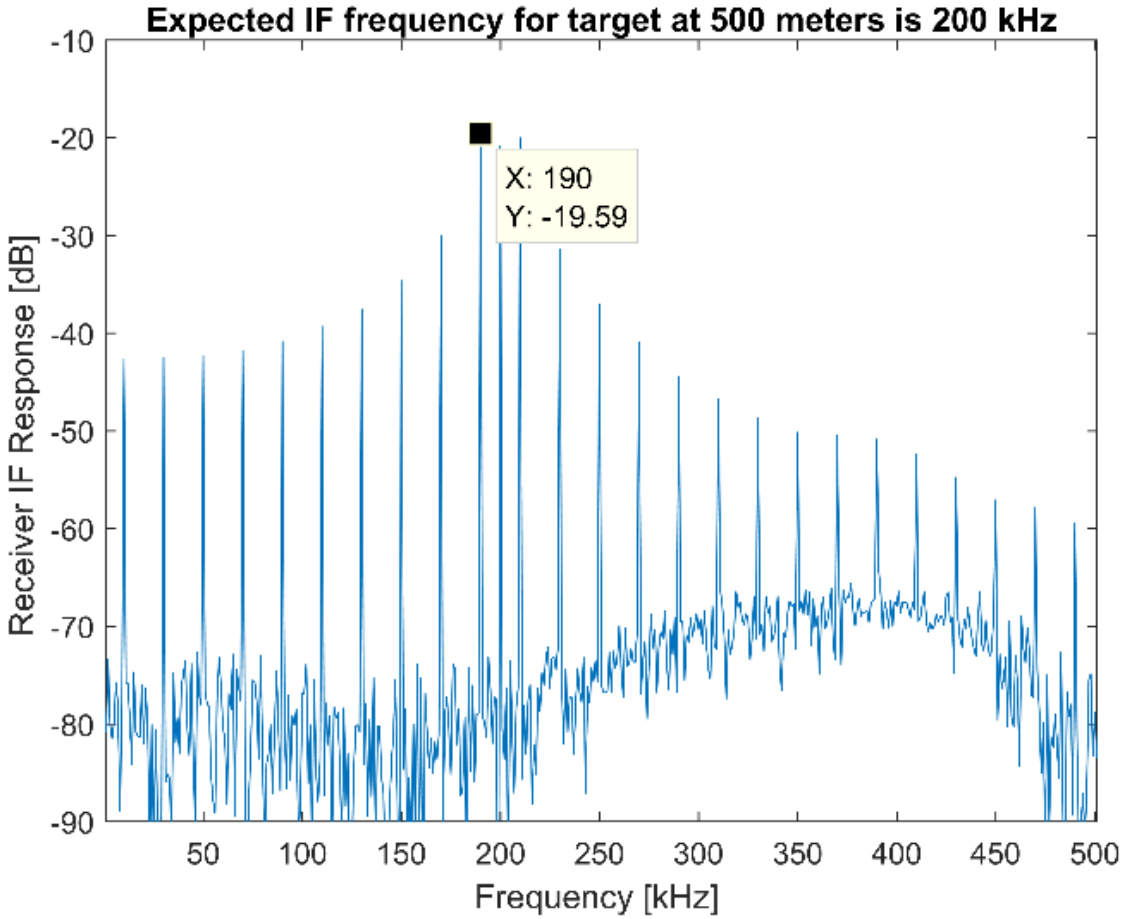
The frequency of IF was calculated and simulated for 1,2,5,10,20,50,100,200,500 and 1000 meters, respectively. Expected and Simulated Maximum IF values obtained as a result of the simulation are shown in Table 5.1.

Distance	**Expected IF Freq**	**Simulated IF Freq**
1	0.4 kHz	10 kHz
2	0.8 kHz	10 kHz
5	2 kHz	10 kHz
10	4 kHz	10 kHz
20	8 kHz	10 kHz
50	20 kHz	10 kHz
100	40 kHz	30 kHz
200	80 kHz	70 kHz
500	200 kHz	190 kHz
1000	400 kHz	390 kHz

Table 5.1 Expected and Simulated Maximum IF values

Example receiver IF Response and frequency measurement are shown in figure 4.1. The range was chosen 500 meters, and the expected IF frequency was calculated according to equation 4.1 and found to be 200 kHz. Although the calculated IF result is 200 kHz, the simulated maximum receiver IF response was observed to occur at 190 kHz with a value of -19.90 dB.

Figure 5.1 Receiver IF Response (dBm) – Frequency Graph



In figure 5.1 above, only 500 meters sample is given, and the calculated and simulated values are explained. The calculated and simulated IF results for other distances in the table are presented in figures 5.2 – 5.11.

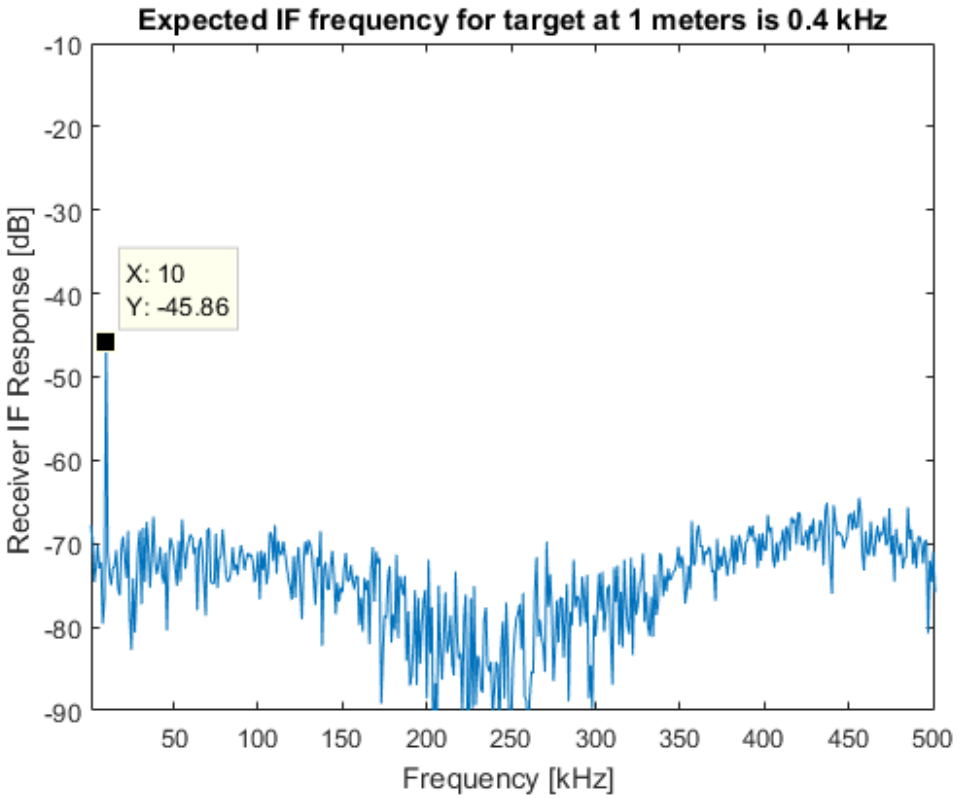


Figure 5.2 Receiver IF Response (dBm) – Frequency Graph @ 1 meter

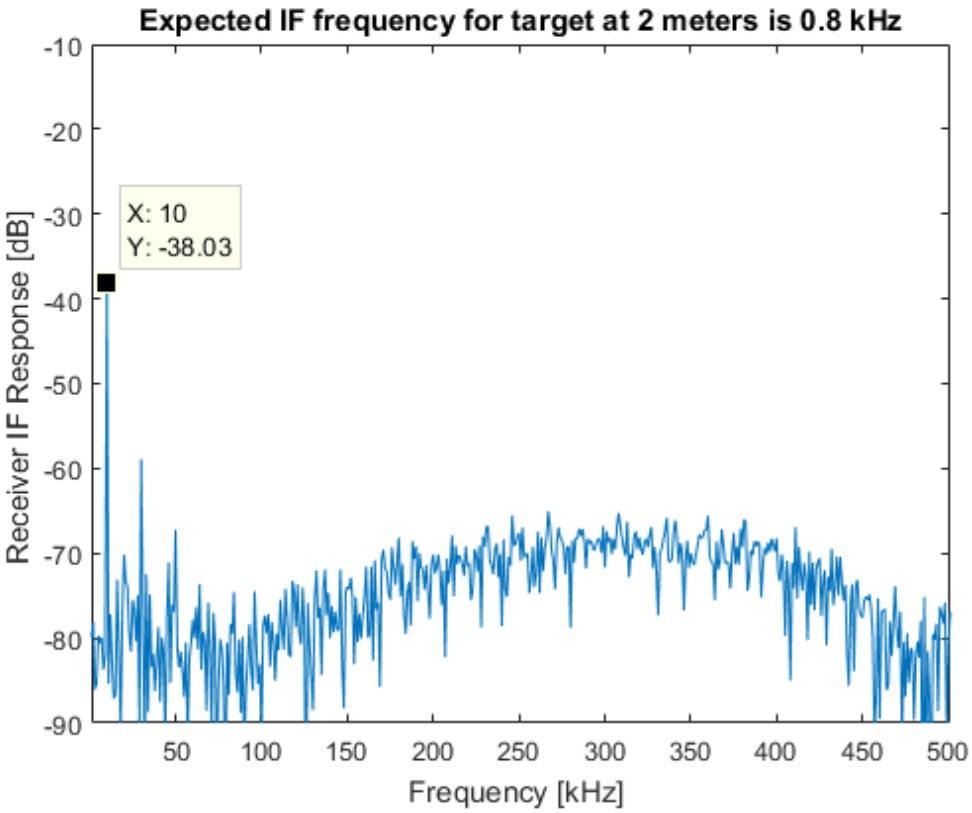


Figure 5.3 Receiver IF Response (dBm) – Frequency Graph @ 2 meters

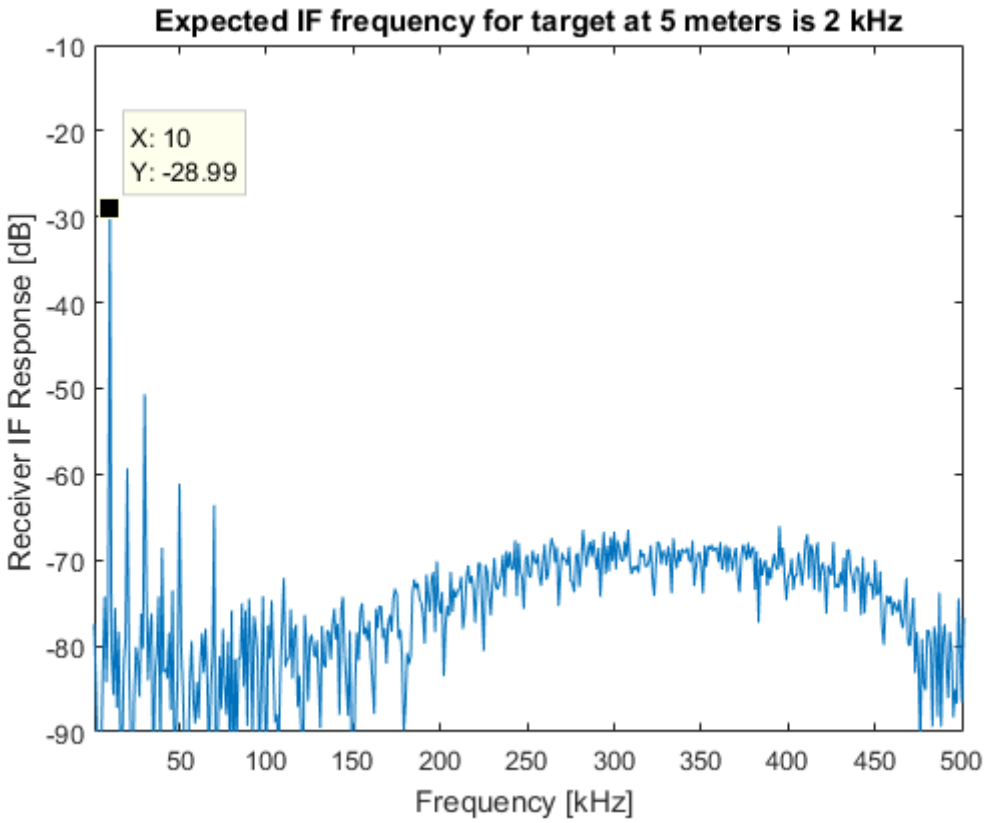


Figure 5.4 Receiver IF Response (dBm) – Frequency Graph @ 5 meters

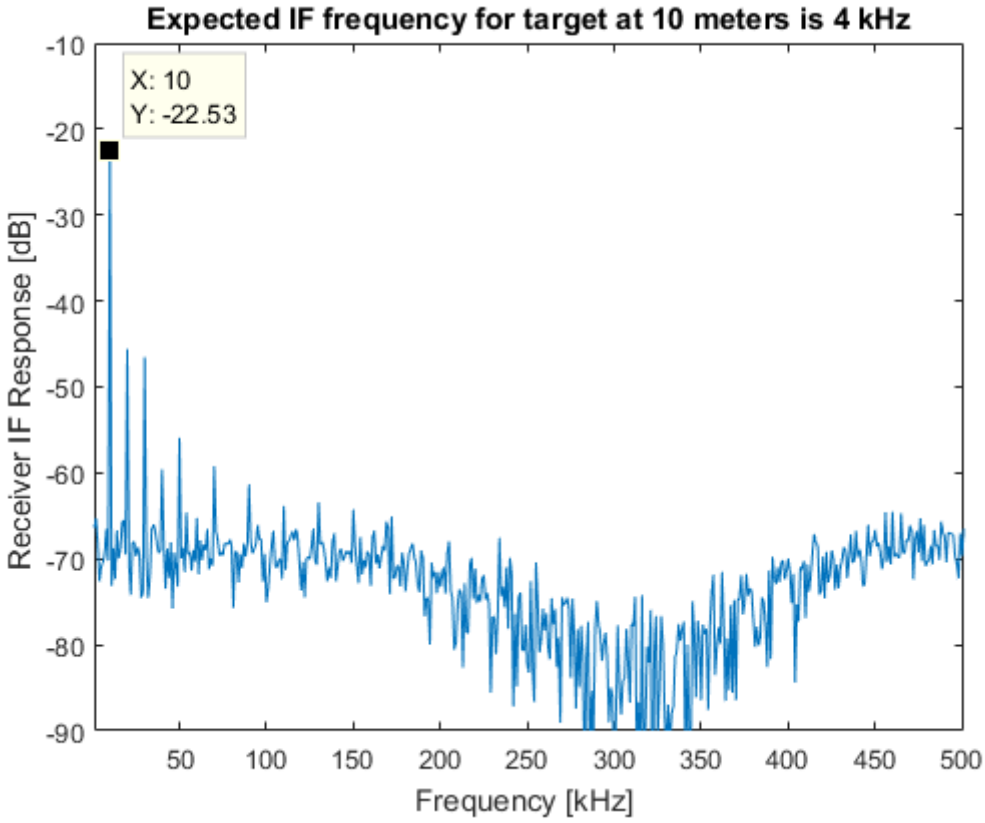


Figure 5.5 Receiver IF Response (dBm) – Frequency Graph @ 10 meters

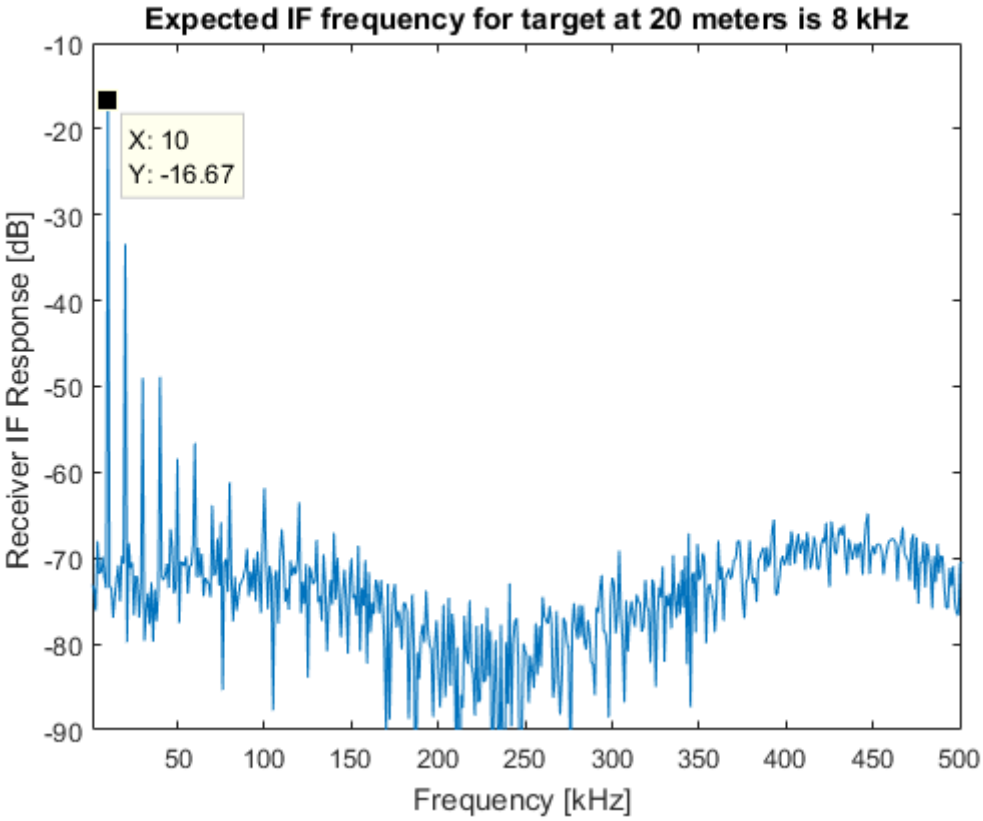


Figure 5.6 Receiver IF Response (dBm) – Frequency Graph @ 20 meters

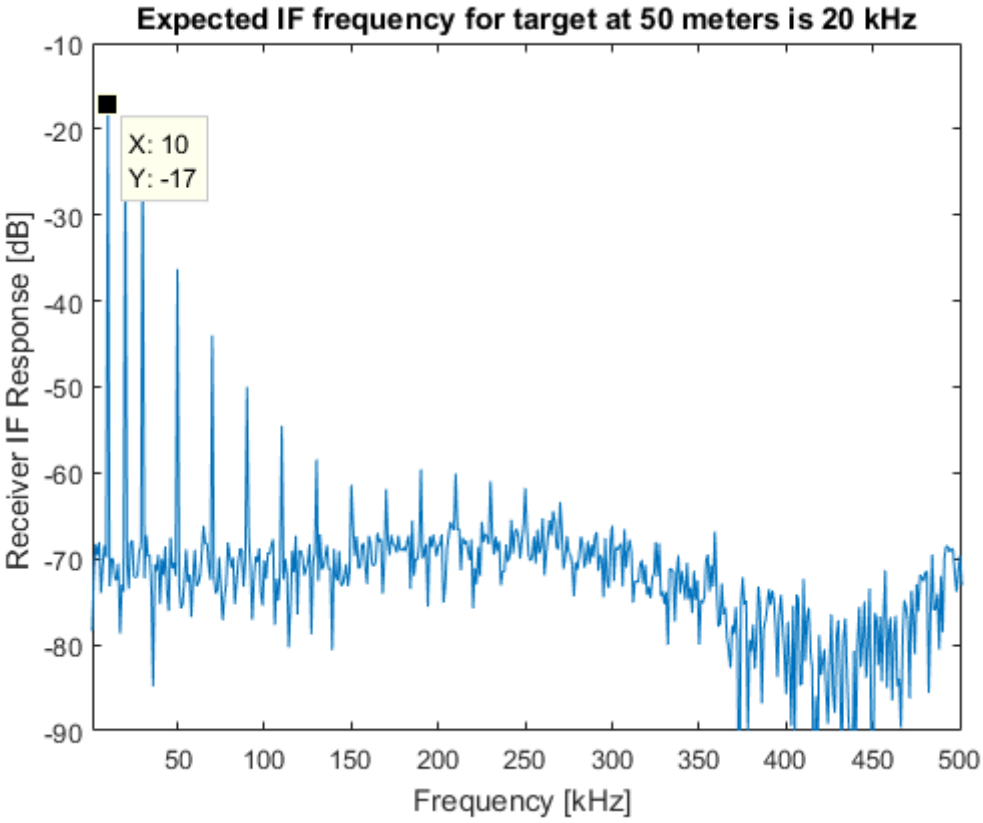


Figure 5.7 Receiver IF Response (dBm) – Frequency Graph @ 50 meters

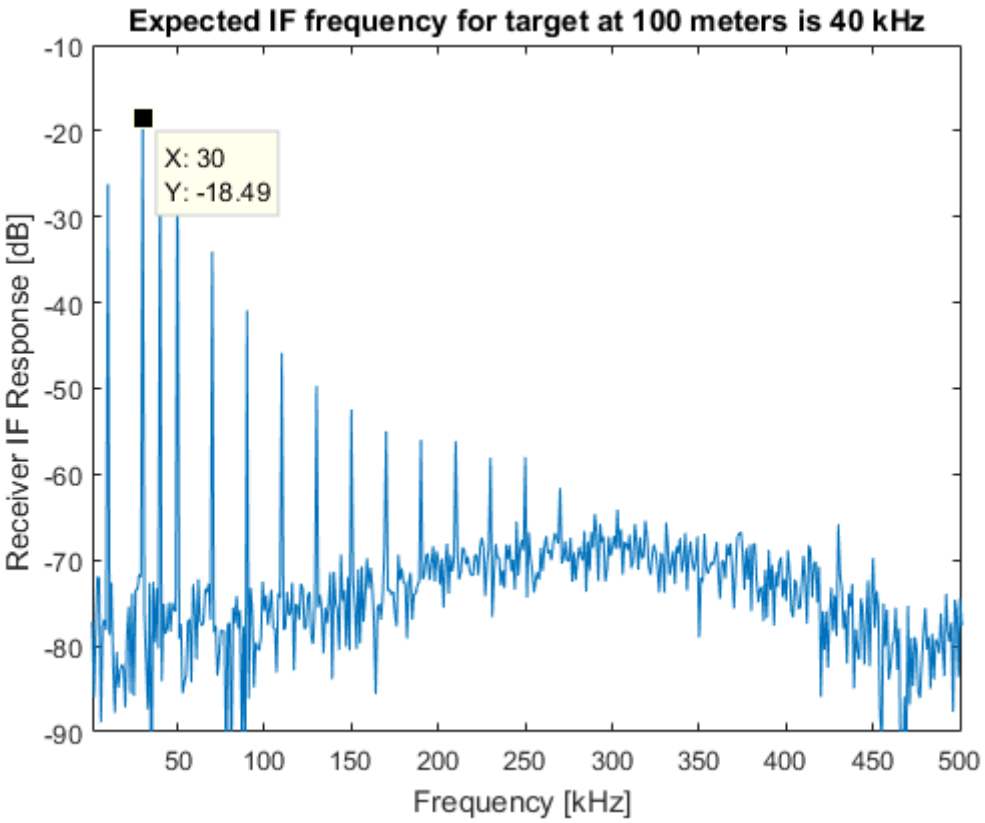


Figure 5.8 Receiver IF Response (dBm) – Frequency Graph @ 100 meters

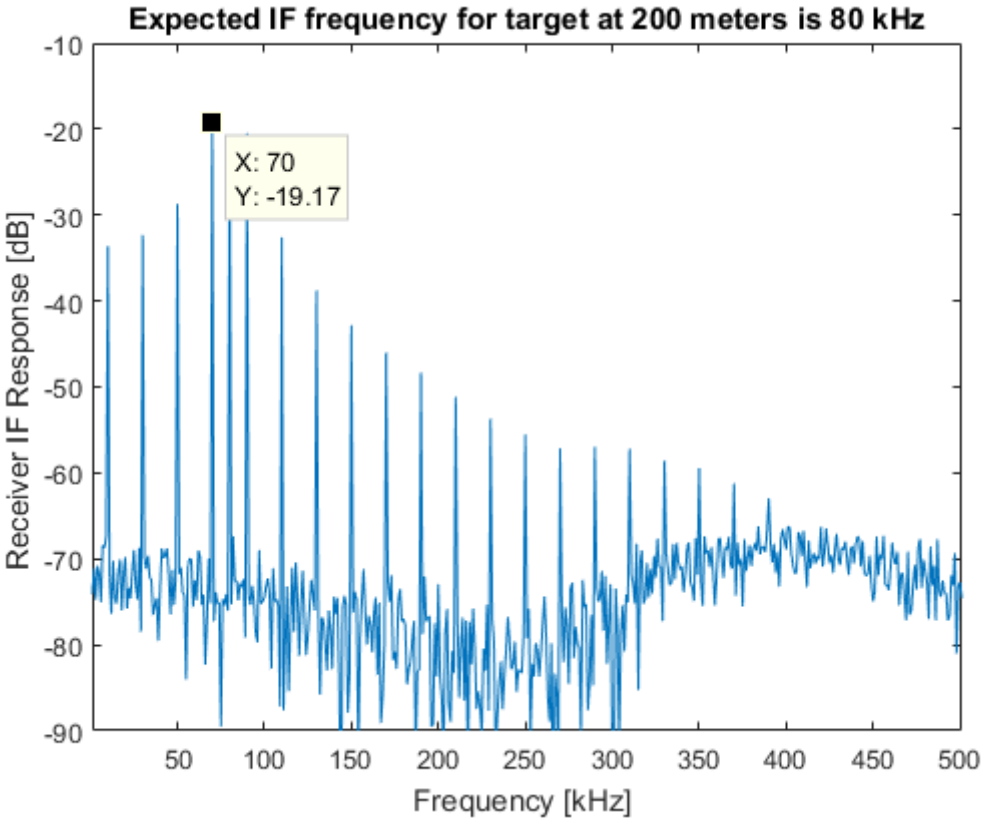


Figure 5.9 Receiver IF Response (dBm) – Frequency Graph @ 200 meters

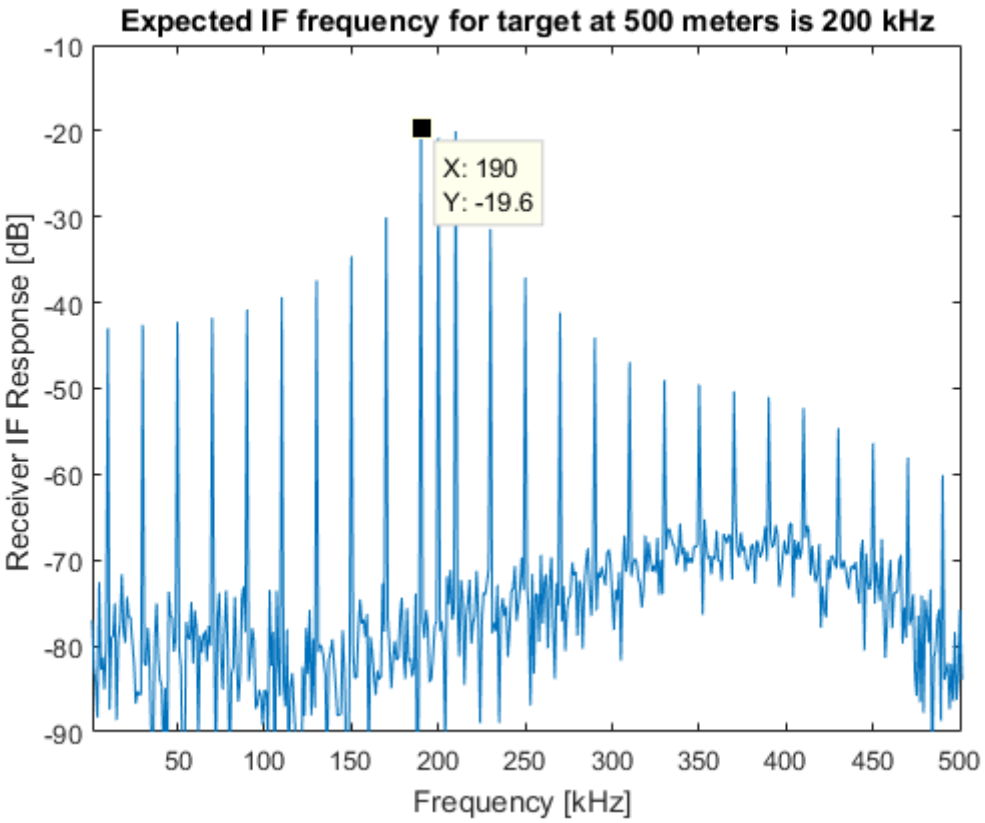


Figure 5.10 Receiver IF Response (dBm) – Frequency Graph @ 500 meters

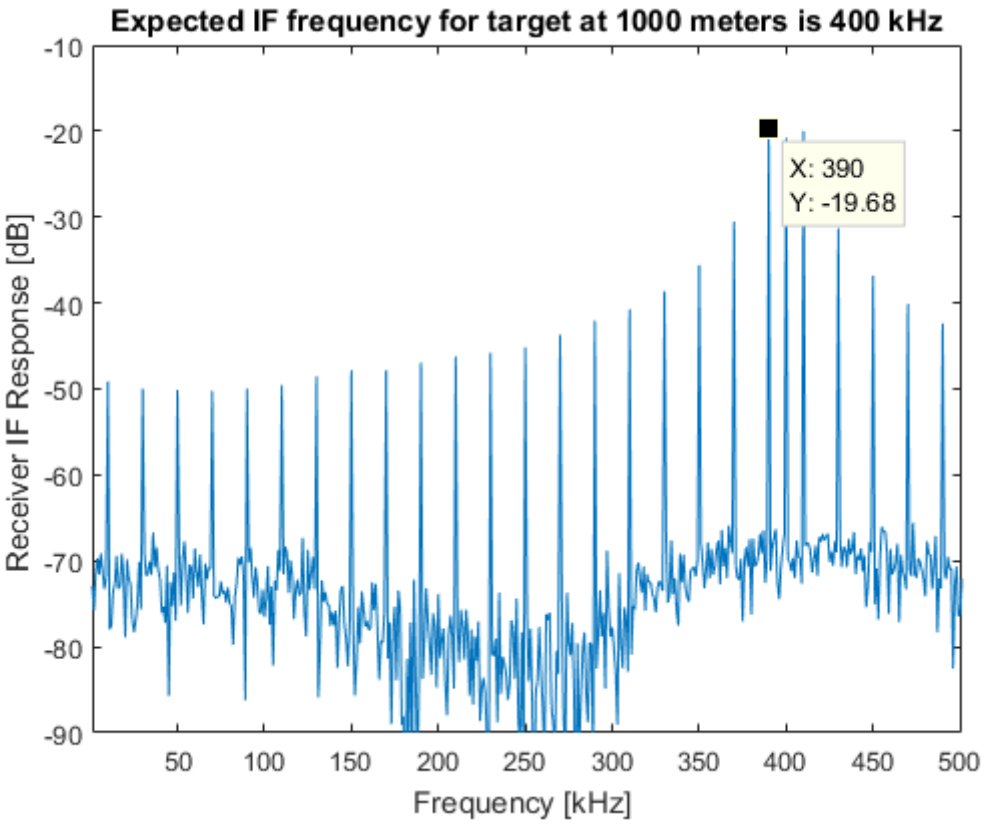


Figure 5.11 Receiver IF Response (dBm) – Frequency Graph @ 1000 meters

According to all specified range values calculated and simulated IF frequency results are presented in figure 5.12.

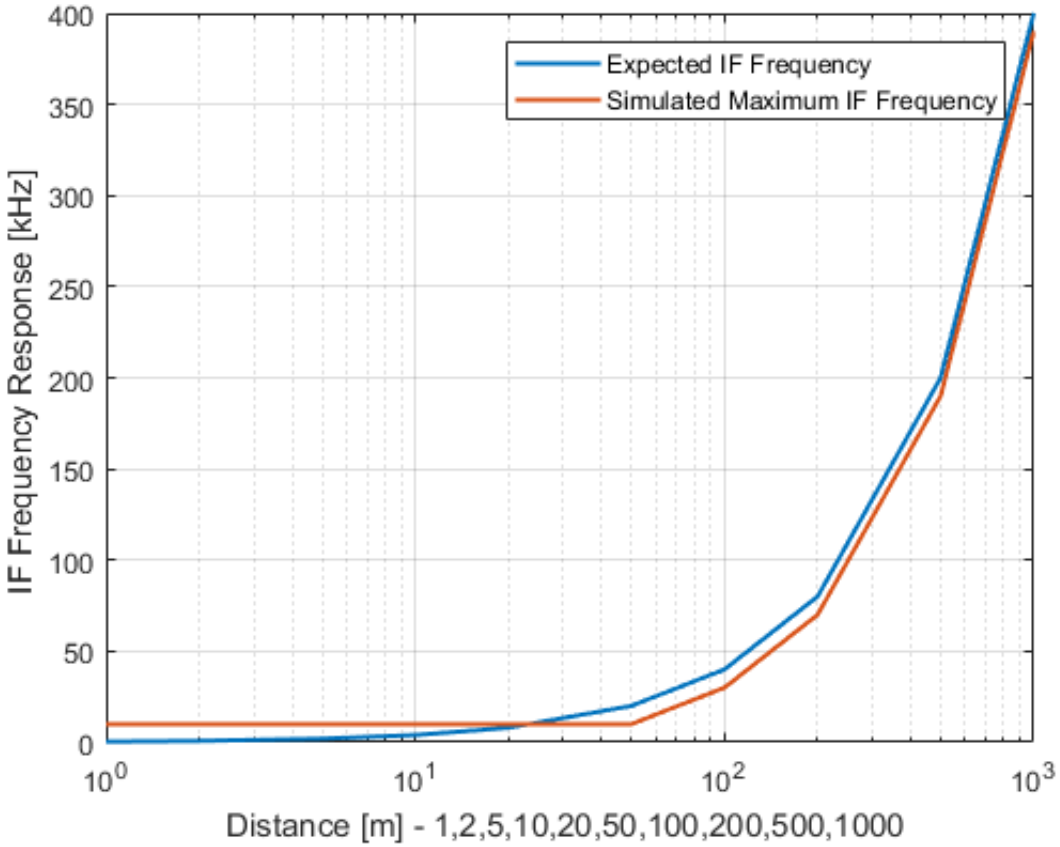


Figure 5.12 Calculated and Simulated Maximum IF Frequency Results

As seen in figure 4.12, there are small differences for each step between the calculated and simulated maximum IF measurements. This indicates that the calculated IF result at the specified range value, overlaps with the simulated maximum IF value. After testing the accuracy of the calculations, measurements were taken on the setup in the laboratory. Since the area in the laboratory is limited, we took measurements at 12 meters. As shown in figure 5.13 and figure 5.14, when the exponential fitting is applied to the 1st and 2nd harmonics in the difference signal, the 3dB point is approximately 5kHz signal is obtained, which corresponds to 12.5 meters. The laboratory measurements show that the distance was measured with an error rate of 4%. With exponential curve fitting, it has been shown that the distances that can cause IF less than 10 kHz can be estimated.

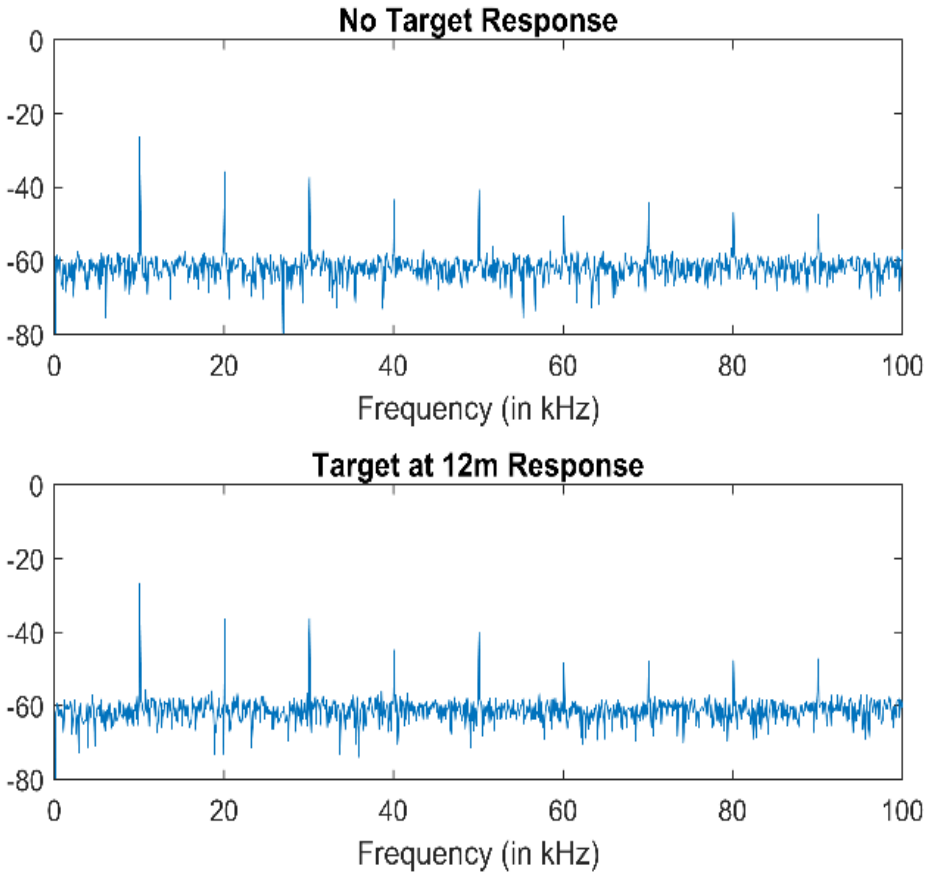


Figure 5.13 Laboratory measurements at 12 meters

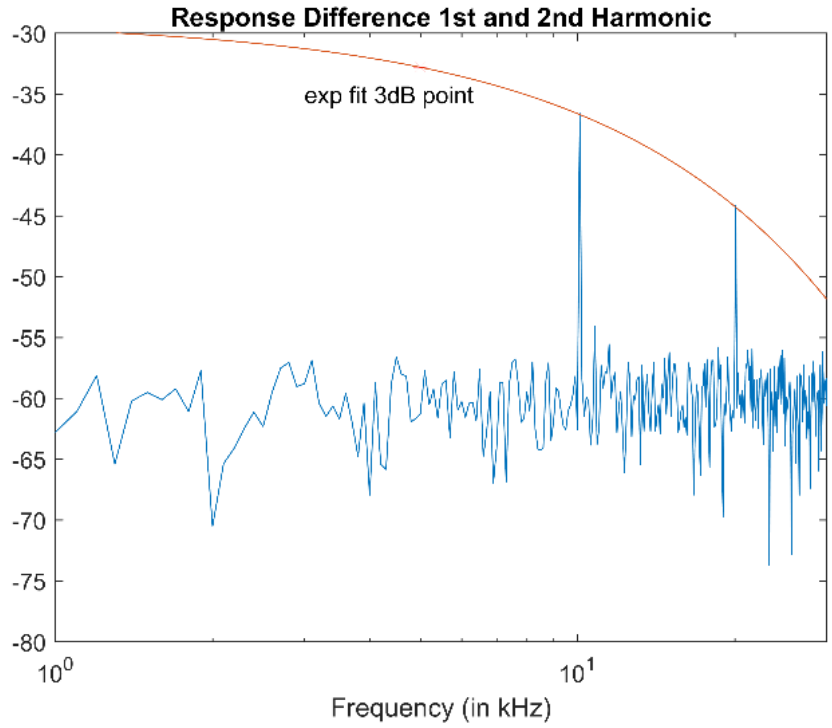


Figure 5.14 Response Difference 1st and 2nd Harmonic

CHAPTER 6

DISCUSSION AND CONCLUSION

It has been emphasized in previous chapters that civilian solutions in PIDS often have low target detection range. In addition, In addition, the distance information of the target cannot be obtained. FMCW (Frequency Modulated Continuous Wave) radars must be used to determine the distance to the target. The cost of these radars, which are more complex than other simple sensors, is higher than other simple radars such as Doppler radar. The ability to detect a target beyond kilometers with such an inexpensive sensor draws attention as a very innovative issue.

In this thesis, it has been shown that the distance information of the target can be obtained by operating the very low-cost Doppler radar sensor according to the FMCW radar principles. According to specified parameters of the sensor, Expected/Simulated IF and range relations were calculated. The simulated and calculated values were confirmed by laboratory measurements. In this way, it has been shown that low-cost perimeter intrusion radar can be developed, and the target's speed and distance information can be obtained using very cheap sensors. Since the sensor's internal receiver antenna is not suitable for target detection from long distances, the lens was designed and placed in front of the sensor receiver to increase the range. It has been shown by calculations that the maximum range value can be increased approximately ten times with the designed external lens

In the future, in order to further increase the target detection range, another lens with different parameters will be designed. In this study, theoretical calculations and simulations are made, and the proof of concept is demonstrated. Next, the sensor will be tested not only under laboratory conditions but also under real conditions. Hardware improvements such as embedded signal processing platforms and precision ADC will be provided to operate the sensor in real conditions on the fence.

REFERENCES

[1] JF Federici, L. Moeller, K. Su, 6 - Terahertz wireless communications, Editor(s): Daryoosh Saeedkia, In Woodhead Publishing Series in Electronic and Optical Materials, Handbook of Terahertz Technology for Imaging, Sensing and Communications, Woodhead Publishing, 2013, Pages 156-214.

[2] Butler, W.a , Poitevin, P.b , Bjornholt, J.a, "Benefits of wide area intrusion detection systems using FMCW radar", Proc. of SPIE 6943, 69430Q (2008).

[3] J.D. Williams, Advanced technologies for perimeter intrusion detection sensors, Security and Detection, 1995, in: European Convention, on,133,137, 16–18 May, 1995.

[4] W. Butler, "Design considerations for intrusion detection wide area surveillance radars for perimeters and borders," IEEE Conf. Tech. Homeland Security, pp. 47-50, May 2008.

[5] Barry, A. S., & Czechanski, J. (2000). Ground surveillance radar for perimeter intrusion detection. In AIAA/IEEE Digital Avionics Systems Conference - Proceedings (Vol. 2). IEEE. https://doi.org/10.1109/dasc.2000.884927.

[6] Meyerhoff, N. J. (2008). New concepts in intrusion detection. In 2008 IEEE International Conference on Technologies for Homeland Security, HST'08 (pp. 63–66). https://doi.org/10.1109/THS.2008.4534424.

[7] Xu, X., Zhao, C., Ye, T., & Gu, T. (2019). Minimum cost deployment of bistatic radar sensor for perimeter barrier coverage. Sensors (Switzerland), 19(2). https://doi.org/10.3390/s19020225.

[8] Hennin, S., Germana, G. & Garcia, L., Integrated perimeter security system. in 2007 IEEE Conference on Technologies for Homeland Security, 2007.

[9] F. Nobis, M. Geisslinger, M. Weber, J. Betz and M. Lienkamp, "A Deep Learning-based Radar and Camera Sensor Fusion Architecture for Object Detection," 2019 Sensor Data Fusion: Trends, Solutions, Applications (SDF), Bonn, Germany, 2019, pp. 1-7.

[10] Fontana, R. J., Foster, L. A., Fair, B., & Wu, D. (2007). Recent advances in Ultra Wideband radar and ranging systems. In 2007 IEEE International Conference on Ultra-Wideband, ICUWB (pp. 19–25). https://doi.org/10.1109/ICUWB.2007.4380908.

[11] E. Ashraf, S. M. Gasser, M. S. El-Mahallawy and M. H. A. ElAzeem, "Performance enhancement of wide-band radar signals, using a new adaptive CAMP algorithm in compressive sensing," 2018 5th International Conference on Electrical and Electronic Engineering (ICEEE), Istanbul, 2018, pp. 366-370.

[12] E. Afacan, B. Saka and E. Yazgan, "Irregular terrain modeling for the low altitude radar applications," Proceedings of MELECON '94. Mediterranean Electrotechnical Conference, Antalya, Turkey, 1994, pp. 387-389 vol.2.

[13] Caruso, M., Meta, A., Corucci, L., & Lombardo, P. (2013). An X-band FMCW radar for airports' perimeter surveillance. In Proceedings International Radar Symposium (Vol. 2, pp. 853–858).

[14] M. Y. A. Abdulrazigh, E. Uzundurukan and A. Kara, "Analysis of Measurement Instrumentation Delay in Modular Experimental Radar at C Band," in Signal Processing and Communications Applications Conference (SIU), 2018 26th, 2018, IEEE.

[15] O. Başarslan and E. Yaldız, "Implementation of FMCW radar for training applications," 2017 4th International Conference on Electrical and Electronic Engineering (ICEEE), Ankara, 2017, pp. 304-308.

[16] Skolnik Merrill I. "Introduction to Radar Systems, Third Ed.", McGraw –Hill Higher Education, 2001, ISBN 0-07-290980-3.

[17] Yılmaz, Hasan Önder. (2018). Metamaterial Antenna Design for 5.8 GHz Doppler Radar. (Master's thesis). Retrieved from https://tez.yok.gov.tr/.

[18] Victor C. Chen. "The Micro-Doppler Effect in Radar, Second Edition", Artech House, 2019, ISBN 9781630815462

[19] HB100 Doppler Radar Module, Agilsense. Accessed: Nov. 30, 22018. [Online]. Available: https://www.agilsense.com, last.

[20] Winkler, V. (2007). Range Doppler detection for automotive FMCW radars. In 2007 European Radar Conference, EURAD (pp. 166–169). https://doi.org/10.1109/EURAD.2007.4404963.

[21] Stove, A. G. (1992). Linear FMCW radar techniques. IEE Proceedings, Part F: Radar and Signal Processing, 139(5), 343–350. https://doi.org/10.1049/ip-f-2.1992.0048.

[22] Kandis, Hamza. (2019). 77 GHz SiGe BiCMOS FMCW RADAR for Automotive Applications (Master's thesis). Retrieved from https://tez.yok.gov.tr/.

[23] Molchanov, Pavlo. (2014). Radar Target Classification by Micro-Doppler Contributions (Doctoral dissertation). Retrieved from https://trepo.tuni.fi/handle/10024/114417.

[24] T. Instruments, "Introduction to mmwave Sensing: FMCW Radars" https://training.ti.com/sites/default/files/docs/mmwaveSensing-FMCW-offlineviewing_0.pdf note = Accessed: 2020-07-24

[25] Antenna Test Lab Company, "Low Cost Microwave Radar Modules Sensor Test Image" https://antennatestlab.com/antenna-examples/radar-antenna-pattern-rcwl-0516-hb100-cdm324 note = Accessed: 2020-07-27

[26] Antenna Test Lab Company, "3D Plotting Spherical Software" https://antennatestlab.com/antenna-education-tutorials/plotting note = Accessed: 2020-07-27

[27] Texas Instruments Company, "An Etendue how-to: A brief introduction to etendue in projection systems" https://training.ti.com/etendue-how-brief-introduction-etendue-projection-systems note = Accessed: 2020-08-25

[28] Light Prescriptions Innovators Company, Oliver Dross, LPI Europe, "Basic Optical Concepts" http://www.lpi-llc.com/Papers/OpticsBasics08.pdf note = Accessed: 2020-08-20

[29] Kim, B. S., Jin, Y., Kim, S., & Lee, J. (2019). A low-complexity FMCW surveillance radar algorithm using two random beat signals. Sensors (Switzerland), 19(3). https://doi.org/10.3390/s19030608

[30] Lee, H., Kim, B. H., Park, J. K., Kim, S. W., & Yook, J. G. (2020). A Resolution enhancement technique for remote monitoring of the vital signs of multiple subjects using a 24 GHz bandwidth-limited fmcw radar. IEEE Access, 8, 1240–1248. https://doi.org/10.1109/ACCESS.2019.2961130.

APPENDICES

Appendix A: IEEE Standard Letter Designations for Radar Bands Used by the EESS Community and Their Comparison to the ITU Allocations

Band Designation	Nominal Frequency Range	Specific Frequency Ranges for Radar Based on ITU Assignments		
		Region 1	Region 2	Region 3
VHF	30-300 MHz	None	138-144 MHz	223-230 MHz
			216-225 MHz	
UHF	300-1000 MHz (Note 5)	420-450 MHz		
		890-942 MHz		
L	1-2 GHz	1215-1400 MHz		
S	2-4 GHz	2300-2500 MHz		
		2700-3600 MHz	2700-3700 MHz	
C	4-8 GHz	4200-4400 MHz		
		5250-5850 MHz	5250-5925 MHz	
X	8-12 GHz		8.5-10.68 GHz	
Ku	12-18 GHz	13.4-14 GHz		
		15.7-17.7 GHz		
K	18-27 GHz	24.05-24.25 GHz	24.05-24.25 GHz	24.05-24.25 GHz
			24.65-24.75 GHz	
Ka	27-40 GHz		33.4-36 GHz	
V	40-75 GHz		59-64 GHz	
W	75-110 GHz		76-81 GHz	
			92-100 GHz	
mm	110-300 GHz		126-142 GHz	
			144-149 GHz	
			231-235 GHz	
			238-248 GHz	

Appendix B: MATLAB Code for IF-Range Simulation

```
clear all; close all;
dist= 1000;% m distance to target
f1=50e6;
deltaf=3e6;
Fsw=10e3;
Tsw=1/Fsw;
Fs=f1*128;
Ts=1/Fs;
t=0:Ts:10*Tsw;
N = length(t);
dF = Fs/N;                  % hertz
f = -Fs/2:dF:Fs/2-dF;       % hertz
fplus=dF:dF:Fs/2-dF;        % hertz
indexplus= round(N/2+1):1:(N-1);
finst=f1+0.5*deltaf*sawtooth(2*pi*Fsw.*t,1/2);
fmcwtx=sin(2*pi*finst.*t);
ToF=2*dist/3e8;
if_freq = 2 * deltaf * Fsw * ToF;
fmcwrx= sin(2*pi*finst.*(t-ToF))+1*randn(1,N);
fmcw_mix=fmcwtx.*fmcwrx;
[b,a] = cheby1(8,3,(f1/Fs/4));
fmcw_if= filter(b,a,fmcw_mix);
T=fftshift(fft(fmcwtx));
R=fftshift(fft(fmcwrx));
Y=fftshift(fft(fmcw_mix));
plot((fplus/1e3),10*log(abs(Y(indexplus)/N)));
xlim ([1 501]);
ylim ([-90 -10]);
xlabel(['Frequency [kHz] ']);
ylabel(['Receiver IF Response [dB] ']);
title(['Expected IF frequency for target at ',num2str(dist),' meters is ',num2str((if_freq/1e3)),'
kHz'])
```

Appendix C: MATLAB Code for Expected and Simulated Maximum IF Frequency

```
clear all; close all;
dist= 1000;% m distance to target
f1=50e6;
deltaf=3e6;
Fsw=10e3;
Tsw=1/Fsw;
Fs=f1*128;
Ts=1/Fs;
t=0:Ts:10*Tsw;
N = length(t);
dF = Fs/N;                  % hertz
f = -Fs/2:dF:Fs/2-dF;       % hertz
fplus=dF:dF:Fs/2-dF;        % hertz
indexplus= round(N/2+1):1:(N-1);
finst=f1+0.5*deltaf*sawtooth(2*pi*Fsw.*t,1/2);
fmcwtx=sin(2*pi*finst.*t);
dist = [1,2,5,10,20,50,100,200,500,1000];
for i=1:length(dist)
  ToF(i)=2*dist(i)/3e8;
  if_freq(i) = (2 * deltaf * Fsw * ToF(i))/1e3;
  fmcwrx= sin(2*pi*finst.*(t-ToF(i)))+1*randn(1,N);
  fmcw_mix=fmcwtx.*fmcwrx;
  [b,a] = cheby1(8,3,(f1/Fs/4));
  fmcw_if= filter(b,a,fmcw_mix);
  T=fftshift(fft(fmcwtx));
  R=fftshift(fft(fmcwrx));
  Y=fftshift(fft(fmcw_mix));
  Y_log = 10*log(abs(Y(indexplus)/N));
  [MaxIFdB(i), MeasuredMaxIF_freq(i)] = max(double(Y_log));
end
semilogx(dist,if_freq,'linewidth',1.5)
hold on
semilogx(dist,MeasuredMaxIF_freq,'linewidth',1.5)
```

```
hold on
grid on
xlabel(['Distance [m] - 1,2,5,10,20,50,100,200,500,1000 ']);
ylabel(['IF Frequency Response [kHz] ']);
legend('Expected IF Frequency','Simulated Maximum IF Frequency')
figure;
stem(dist,if_freq,'filled','linewidth',1.5 )
hold on
stem(dist,MeasuredMaxIF_freq,'filled','linewidth',1.5 );
grid on
xlabel(['Distance [m] - 1,2,5,10,20,50,100,200,500,1000 ']);
ylabel(['IF Frequency Response [kHz] ']);
legend('Expected IF Frequency','Simulated Maximum IF Frequency')
```

Appendix D: MATLAB Code for Laboratory Measurements at 12 meters

```
clear all; close all;
load tek_data.mat
t = data(:,1);
dt=t(2)-t(1);
Fs=1/dt;
N = length(t);
%% Sine wave:
x = data(:,2);
y=data(:,3);
x=x-mean(x);%
y=y-mean(y);%
%% Fourier Transform:
X = fftshift(fft(x));
Y = fftshift(fft(y));
Z = fftshift(fft(y-x));
%% Frequency specifications:
dF = Fs/N;                  % hertz
f = -Fs/2:dF:Fs/2-dF;          % hertz
fplus=dF:dF:Fs/2-dF;          % hertz
indexplus= round(N/2+1):1:(N-1);
%% Plot the spectrum:
figure;
subplot(2,1,1);plot(fplus/1e3,10*log10(abs(X(indexplus)/N)));
xlabel('Frequency (in kHz)');
title('No Target Response');
xlim([0 100]);ylim([-80 0]);
subplot(2,1,2);plot(fplus/1e3,10*log10(abs(Y(indexplus)/N)));
xlabel('Frequency (in kHz)');
title('Target at 12m Response');
xlim([0 100]);ylim([-80 0]);
figure;semilogx(fplus/1e3,10*log10(abs(Z(indexplus)/N)));
xlabel('Frequency (in kHz)');
title('Response Difference 1st and 2nd Harmonic');
```

```
xlim([1 30]);ylim([-80 -30]);
filt_resp=10*log10(1*exp(-fplus./5.7e3))-29;
hold;
semilogx(fplus/1e3,filt_resp);
semilogx(fplus(50)/1e3,filt_resp(50),'r*')
xt = 3;
yt = -35;
str = 'exp fit 3dB point';
text(xt,yt,str)
```